Article

Exact Solutions and Cosmological Constraints in Fractional Cosmology

Esteban González [1], Genly Leon [2,3,*] and Guillermo Fernandez-Anaya [4]

1   Dirección de Investigación y Postgrado, Universidad de Aconcagua, Pedro de Villagra 2265, Vitacura, Santiago 7630367, Chile; esteban.gonzalez@uac.cl
2   Departamento de Matemáticas, Universidad Católica del Norte, Avda. Angamos 0610, Casilla 1280, Antofagasta 1270709, Chile
3   Institute of Systems Science, Durban University of Technology, P.O. Box 1334, Durban 4000, South Africa
4   Departamento de Física y Matemáticas, Universidad Iberoamericana Ciudad de México, Prolongación Paseo de la Reforma 880, Mexico City 01219, Mexico; guillermo.fernandez@ibero.mx
*   Correspondence: genly.leon@ucn.cl

Abstract: This paper investigates exact solutions of cosmological interest in fractional cosmology. Given μ, the order of Caputo's fractional derivative, and w, the matter equation of state, we present specific exact power-law solutions. We discuss the exact general solution of the Riccati Equation, where the solution for the scale factor is a combination of power laws. Using cosmological data, we estimate the free parameters. An analysis of type Ia supernovae (SNe Ia) data and the observational Hubble parameter data (OHD), also known as cosmic chronometers, and a joint analysis with data from SNe Ia + OHD leads to best-fit values for the free parameters calculated at 1σ, 2σ and 3σ confidence levels (CLs). On the other hand, these best-fit values are used to calculate the age of the Universe, the current deceleration parameter (both at 3σ CL) and the current matter density parameter at 1σ CL. Finding a Universe roughly twice as old as the one of ΛCDM is a distinction of fractional cosmology. Focusing our analysis on these results, we can conclude that the region in which $\mu > 2$ is not ruled out by observations. This parameter region is relevant because fractional cosmology gives a power-law solution without matter, which is accelerated for $\mu > 2$. We present a fractional origin model that leads to an accelerated state without appealing to Λ or dark energy.

Keywords: fractional calculus; cosmological data; cosmology

1. Introduction

In fractional calculus, the classical derivatives and integrals of integer order are generalized to derivatives and integrals of arbitrary (real or complex) order [1–9]. Fractional derivatives have attracted increasing attention because they universally appear as empirical descriptions of complex social and physical phenomena. Fractional calculus applications have grown enormously in recent years because these operators have memory and are more flexible in describing the dynamic behavior of phenomena and systems using fractional differential equations, while the description with integer order differential equations uses local operators and they are limited in the order of differentiation to a constant. Consequently, the resulting models must be sufficiently precise in many cases [10]. Research into fractional differentiation is inherently multi-disciplinary and has applications across various disciplines, for example, fractional quantum mechanics and gravity for fractional spacetime [11,12] and fractional quantum field theory [13–18]. Such frameworks have been essential in understanding complex systems in classical and quantum regimes [19–29].

Regarding the classical regime, fractional derivative cosmology has been established by two methods: (i) The last-step modification method is the simplest one, in which the corresponding fractional field equations replace the given cosmological field equations for a specific model. (ii) The first-step modification method can be considered a more

fundamental methodology. In this method, one starts by establishing a fractional derivative geometry. More concretely, the variational principle for fractional action is applied to establish a modified cosmological model.

Fractional calculus has recently been explored to address problems related to cosmology in [27,30–62]. For example, in [30,34], the Riemann curvature and the Einstein tensor are defined as usual, but now with dependence on the μ fractional parameter. Then, it is possible to write a fractional analogous to the Einstein field equation through the expression $G_{\alpha\beta}(\mu) = 8\pi G T_{\alpha\beta}(\mu)$, where $G_{\alpha\beta}(\mu)$ is the Einstein tensor in fractional calculus and G is the Newton gravitational constant. These studies correspond to the last-step modification method, as mentioned above. Modifications to several astrophysical and cosmological events can be studied based on the last equation. For example, a fractional theory of gravitation for fractional spacetime has been developed in [31,32]. Non-holonomic deformations to cosmology lead to new classes of cosmological models, which have been studied in [33,57].

In reference [61], a joint analysis using data from cosmic chronometers and type Ia supernovae was performed. This comparison with observational tests was used to find best-fit values for the fractional order of the derivative. These methods are a robust scheme for investigating the physical behavior of cosmological models [61,63–66] and can be used in new contexts, such as in [62], where dynamical systems and phase spaces were used to analyze fractional cosmology for different matter contents, obtaining a late-time accelerating cosmology.

Undeniably, the late-time acceleration in the Universe expansion is one of the most challenging topics in modern cosmology.

Since 1998, when the independent projects High-z Supernova Search Team [67] and Supernova Cosmology Project [68] obtained results that suggested this behavior in the Universe, the type Ia supernovae (SNe Ia) data have become a definitive proof to study this era of the Universe and the transition between the decelerated expansion phase and the accelerated one. However, the latter is usually model dependent [69]. In this sense, the observational Hubble parameter data (OHD), also known as cosmic chronometers, have become a fundamental data test, complementary to the SNe Ia data, to study the Universe's expansion rate in a model-independent way. Finally, using these cosmological data, we estimate the free parameters (α_0, μ).

This research's main objective is to investigate open problems in gravity and cosmology. Therefore, we estimate the free parameters using cosmological data. The analysis of the type Ia supernovae (SNe Ia) data and the observational Hubble parameter data (OHD), also known as cosmic chronometers, and the joint analysis of SNe Ia data + OHD lead to best-fit values for the free parameters calculated at the 1σ, 2σ and 3σ confidence levels (CLs). On the other hand, these best-fit values are used to calculate the age of the Universe, the current deceleration parameter (both at the 3σ CL) and the current matter density parameter at 1σ CL. Finding that the Universe is roughly twice as old as the one of ΛCDM is a distinction of fractional cosmology; apart from that, it leads to an accelerated state without appealing to Λ or dark energy. We confirm that this result, which is in disagreement with the value obtained with globular clusters with a value of $t_0 = 13.5^{+0.16}_{-0.14} \pm 0.23$ [70], is a distinction of fractional cosmology. This result also agrees with the analysis performed in ([61], Section 5, page 4817). Despite the discrepancy between the age of the Universe and that determined by globular clusters, it is essential to highlight that fractional cosmology contributes to the solutions to other problems associated with the ΛCDM model, for example, late-time acceleration without dark energy, as we explained before. In this sense, the non-inclusion of a cosmological constant (CC) or some DE can alleviate some other problems related to these components. One of these problems is the so-called CC problem, in which the observational value of the CC differs between 60 and 120 orders of magnitude compared with the value anticipated by particle physics [71–75]. Another problem related to the DE is the coincidence problem, which stipulates that, currently, we are living in an extraordinary epoch in the cosmic evolution, in which DM and DE densities are of the same

order of magnitude, with a fine-tuning problem associated with the context of the ΛCDM model [76–78].

Another issue that fractional cosmology can possibly alleviate is the Hubble tension. Measurements of the Hubble parameter at the current time, H_0, exhibit a discrepancy of 5σ between the observational value obtained from the Hubble Space Telescope (HST) [79] and the one inferred from Planck CMB [80]. The first corresponds to model-independent measurements, while the second depends on the ΛCDM model. According to Riess et al. [81], observational issues such as the H_0 tension are strong evidence that physics beyond the ΛCDM model is required. Therefore, and following this line, a possible alternative to solve this tension considers extensions beyond ΛCDM (see Di Valentino et al. [82] for a review). In [61], some results were discussed related to the H_0 tension in the context of fractional cosmology, and a trend of H_0 to the value obtained by SH0ES [81] at current times was observed, in agreement with Planck's value [80] for $z \lesssim 1.5$. However, the H_0 tension is not fully resolved in the region $1.5 < z < 2.5$.

Moreover, prospects for the density perturbation growth and cosmological structure formation could be described in this context. For example, in [83], it was shown that in the ΛCDM cosmology, the perturbations do not change the stability of the late-time attractor of the background equations and the system still results in the dark-energy-dominated de Sitter solution, with a dark matter era transition and a growth index of $\gamma \approx 6/11$. Here, γ is defined through the relation $d \ln \delta_m / d \ln a \approx \Omega_m^\gamma$, where δ_m is the matter contrast and Ω_m is the fractional energy density of matter. This result for the linear growth rate, $d \ln \delta_m / d \ln a \approx \Omega_m^\gamma$, was corrected to $d \ln \delta_m / d \ln a \approx \Omega_m^{\frac{6}{11}} - \frac{1}{70}(1 - \Omega_m)^{\frac{5}{2}}$ in [84]. In fractional cosmology, the dimensionless energy density of dust matter depends on t through $\Omega_{m,\mu} = \Omega_m \times t^{-(\mu-1)}$; thus, the growth index γ in the matter-dominated solution should be different to $6/11$. In addition, it could be exciting to investigate and try fractional cosmology within a very early universe, fitting data and determining the impact of the fractional derivative term on primordial nucleosynthesis. Fractional cosmology ingredients may enhance inflation, raising the question whether it is possible that issues such as the cosmic no-hair conjecture, isotropization, etc., could be solved [85–91].

According to previous statements, it is essential to see if fractional calculus or fractional cosmology can well-describe the observational data. Then, we can perform more sophisticated calculations to describe the late-time Universe or the very early Universe. Therefore, one can argue that the Universe can be better described with a fractional derivative, not just to fit the data but also to describe the fundamental dynamics, highlighting the demand for new physics. These approaches can help to understand the Universe's acceleration with the mathematical background of fractional calculus. The mathematical richness generated by the corrections due to the fractional index μ of the fractional derivative can resolve the previous problems in future studies. Indeed, we can examine these topics in a forthcoming series of manuscripts with applications in inflation and dark energy models, investigating the physical implications and producing observational constraints.

In this paper, we investigate exact solutions of cosmological interest in fractional cosmology. In particular, we study the cosmological applications of power-law solutions of the type $a = (t/t_0)^{\alpha_0}$, where $\alpha_0 = t_0 H_0$ is the current age parameter. Additionally, given μ, the order of Caputo's fractional derivative, and w, the equation of state (EoS) of matter, one must impose two compatibility conditions which allow particular solutions to (μ, w). Moreover, we are interested in an exact solution that gives the general solution of the system. For this purpose, one can solve the Riccati equation independent of the EoS, where the solution for the scale factor is a combination of power-law solutions. Additionally, we investigate if the solutions take account of the current late-time acceleration.

The paper is organized as follows. Section 2 discusses the basics of the fractional variational approach to cosmology and presents the cosmological equations for a perfect fluid. In Section 2.3, we comment on the crucial difference between fractional and standard cosmology; that is, we obtain late-time acceleration without adding a cosmological constant, quintessence scalar field or other exotic fluids as compared to standard cosmology.

In Section 2.5, we consider a model with cold dark matter to present a specific realization of these possibilities and we interpret the fractional modification as dark energy in Section 2.6. Section 3 is devoted to finding exact solutions for the Hubble factor in this scenario. They correspond mainly to power-law solutions for the scale factor and a combination of power-law functions. In Section 3.4, we provide a precise scheme to find approximated analytical solutions to aid in the asymptotic analysis. A discussion is presented in Section 3.5. We solve Bernoulli's equation using differential inequalities and asymptotic expansions to estimate $H(z)$ in redshift. A physical discussion of the results is presented in Section 3.6. In Section 4, a joint analysis using OHD and type Ia supernovae data is performed. This comparison with observational tests was used to find best-fit values for the fractional order of the derivative and the current age parameter α_0. Section 5 is the conclusion.

2. Fractional Action Integral

Recently, a wide range of definitions of fractional derivatives [92], such as the Riemann–Liouville derivative (RLD) and the Caputo derivative (CD), among others, have been used in many applications.

2.1. Some Fractional Derivatives

The RLD with $\mu \geq 0$ for $f(t)$ is defined by

$$D_t^\mu f(t) = \Gamma(n-\mu)^{-1} \frac{d^n}{dt^n} \int_c^t \frac{f(\tau)}{(t-\tau)^{\mu-n+1}} d\tau,$$ (1)

where $n = [\mu] + 1$ and $\mu \in (n-1, n)$.

Note that the main parameter of fractional calculus is given by μ, recovering standard calculus when $\mu \to 1$.

The Caputo left derivative is defined as

$$^C D_t^\mu f(t) = \Gamma(n-\mu)^{-1} \int_c^t \frac{\frac{d^n}{d\tau^n} f(\tau)}{(t-\tau)^{\mu-n+1}} d\tau,$$ (2)

where $n = \begin{cases} [\mu] + 1 & \mu \notin \mathbb{N} \\ \mu & \mu \in \mathbb{N} \end{cases}$. In fractional calculus, we now have the following relation (see [92]) for the case of more than one derivative:

$$D_t^\mu \left[D_t^\beta f(t) \right] = D_t^{\mu+\beta} f(t) - \sum_{j=1}^n D_t^{\beta-j} f(c+) \frac{(t-c)^{-\mu-j}}{\Gamma(1-\mu-j)},$$ (3)

or in other words $D_t^\mu D_t^\beta f(t) \neq D_t^{\mu+\beta} f(t)$, if not all derivatives $D_t^{\beta-j} f(c+)$ are equal to zero at c. Additionally, the fractional derivative of the Leibniz rule [92] reads as

$$D_t^\mu [f(t)g(t)] = \sum_{k=0}^\infty \frac{\Gamma(\mu+1)}{k!\Gamma(\mu-k+1)} D_t^{\mu-k} f(t) D_t^k g(t),$$ (4)

having the usual when $\mu = n \in \mathbb{N}$.

2.2. Frational Action-like Variational Problems

Within the first-step modification method, one procedure uses the fractional variational approach developed in [30,93–97] with the following fractional action integral,

$$S(\tau) = \frac{1}{\Gamma(\mu)} \int_0^\tau \mathcal{L}(\theta, q_i(\theta), \dot{q}_i(\theta), \ddot{q}_i(\theta))(\tau-\theta)^{\mu-1} d\theta,$$ (5)

where $\Gamma(\mu)$ is the Gamma function, $\mathcal{L}$ is the Lagrangian, μ is the constant fractional parameter and τ and θ are the observers and intrinsic time, respectively, and the action integral depends on second order derivatives of the generalized coordinates q_i.

Variation in (5) with respect to q_i leads to the Euler–Poisson equations [97]:

$$
\begin{aligned}
&\frac{\partial \mathcal{L}(\theta, q_i(\theta), \dot{q}_i(\theta), \ddot{q}_i(\theta))}{\partial q_i} - \frac{d}{d\theta}\frac{\partial \mathcal{L}(\theta, q_i(\theta), \dot{q}_i(\theta), \ddot{q}_i(\theta))}{\partial \dot{q}_i} + \frac{d^2}{d\theta^2}\frac{\partial \mathcal{L}(\theta, q_i(\theta), \dot{q}_i(\theta), \ddot{q}_i(\theta))}{\partial \ddot{q}_i} \\
&= \frac{1-\mu}{\tau-\theta}\left(\frac{\partial \mathcal{L}(\theta, q_i(\theta), \dot{q}_i(\theta), \ddot{q}_i(\theta))}{\partial \dot{q}_i} - 2\frac{d}{d\theta}\frac{\partial \mathcal{L}(\theta, q_i(\theta), \dot{q}_i(\theta), \ddot{q}_i(\theta))}{\partial \ddot{q}_i} \right) \\
&\quad - \frac{(1-\mu)(2-\mu)}{(\tau-\theta)^2}\frac{\partial \mathcal{L}(\theta, q_i(\theta), \dot{q}_i(\theta), \ddot{q}_i(\theta))}{\partial \ddot{q}_i}.
\end{aligned}
\tag{6}
$$

2.3. Applications to Cosmology

In cosmology, it is assumed that the flat Friedmann provides the geometry of spacetime Lemaître–Robertson–Walker (FLRW) metric:

$$
ds^2 = -N^2(t)dt^2 + a^2(t)(dx^2 + dy^2 + dz^2),
\tag{7}
$$

where $a(t)$ denotes the scale factor and $N(t)$ is the lapse function. This result is based on Planck's observations [80].

For the metric (7), the Ricci' scalar depends on the second derivatives of a and first derivatives of N and reads

$$
R(t) = 6\left(\frac{\ddot{a}(t)}{a(t)N^2(t)} + \frac{\dot{a}^2(t)}{a^2(t)N^2(t)} - \frac{\dot{a}(t)\dot{N}(t)}{a(t)N^3(t)} \right).
\tag{8}
$$

Consider the point-like action integral

$$
S(\tau) = \int_0^\tau \left[\frac{R(\theta)}{2} + L(\theta) \right] a^3(\theta)N(\theta)d\theta,
\tag{9}
$$

where $R(\theta)$ is the Ricci scalar (8). In cosmology, the Einstein–Hilbert Lagrangian density is related to the Ricci scalar. Generically, one takes integration by parts, such that a total derivative is removed for the action, and the derivatives $\ddot{a}(t)$ and $\dot{N}(t)$ are eliminated. We will use a fractional version of the Lagrangian (9); thus, we do not follow the standard procedure and keep the higher order derivatives and use formulation (5) leading to the Euler–Poisson Equation (6). We use fractional variational calculus with classical and Caputo derivatives.

For simplicity, we consider units in which $8\pi G = c = 1$ and assume a perfect fluid for the matter content of the Universe, where $L(\theta) = -\rho_0 a(\theta)^{-3(1+w)}$ for $w \neq -1$ is the usual matter Lagrangian of a perfect fluid as in [98–100] and contains integer-order derivatives in the Lagrangian. We consider the transition to the effective fractional action used in [61], i.e.,

$$
S_{\text{eff}}(\tau) = \frac{1}{\Gamma(\mu)} \int_0^\tau \left[\frac{R(\theta)}{2} + \mathcal{L}(\tau, \theta) \right] (\tau-\theta)^{\mu-1} a^3(\theta)N(\theta)d\theta,
\tag{10}
$$

where $\Gamma(\mu)$ is the Gamma function, $\mathcal{L}(\tau, \theta) = L(\theta)(\tau-\theta)^{-(\mu-1)(w+1)}$, which recovers the usual matter Lagrangian of a perfect fluid as $\mu \to 1$ [98–100], μ is the constant fractional parameter and τ and θ are the observers and intrinsic time, respectively [34]. $w = p/\rho$ is a constant EoS for matter.

For a fixed τ, the expressions

$$
\rho(\theta) = \rho_0 a(\theta)^{-3(1+w)}(\tau-\theta)^{-(\mu-1)(w+1)},
\tag{11}
$$

and

$$
p(\theta) = w\rho_0 a(\theta)^{-3(1+w)}(\tau-\theta)^{-(\mu-1)(w+1)},
\tag{12}
$$

define the energy density and the isotropic pressure of the matter fields. Then,

$$\dot{\rho}(\theta) = \frac{d}{d\theta}\left[\rho_0 a(\theta)^{-3(1+w)}(\tau-\theta)^{-(\mu-1)(w+1)}\right] = (w+1)\rho(\theta)\left(-\frac{3\dot{a}(\theta)}{a(\theta)} - \frac{\mu-1}{\theta-\tau}\right)$$

$$= -3\left(\frac{\dot{a}(\theta)}{a(\theta)} + \frac{1-\mu}{3(\tau-\theta)}\right)(\rho(\theta)+p(\theta)). \tag{13}$$

Defining $q_i \in \{N, a\}$ in (5) for a fixed τ, we have the Lagrangian

$$\mathcal{L}\big(\theta, N(\theta), \dot{N}(\theta), a(\theta), \dot{a}(\theta), \ddot{a}(\theta)\big) :=$$
$$\frac{3a(\theta)\big(N(\theta)\big(a(\theta)\ddot{a}(\theta) + \dot{a}^2(\theta)\big) - a(\theta)\dot{a}(\theta)\dot{N}(\theta)\big)}{N^2(\theta)} - \rho_0 N(\theta)a(\theta)^{-3w}(\tau-\theta)^{-(\mu-1)(w+1)}. \tag{14}$$

The Euler–Poisson Equations (6) obtained after varying the action (10) for $q_i \in \{N, a\}$ lead to the field equations

$$\left(\frac{\dot{a}(\theta)}{a(\theta)}\right)^2 + \frac{(1-\mu)}{(\tau-\theta)}\frac{\dot{a}(\theta)}{a(\theta)} = \frac{1}{3}\rho_0 a(\theta)^{-3(1+w)}(\tau-\theta)^{-(\mu-1)(w+1)}, \tag{15}$$

$$\frac{\ddot{a}(\theta)}{a(\theta)} + \frac{1}{2}\left(\frac{\dot{a}(\theta)}{a(\theta)}\right)^2 + \frac{(1-\mu)}{(t-\theta)}\frac{\dot{a}(\theta)}{a(\theta)} + \frac{(\mu-2)(\mu-1)}{2(\tau-\theta)^2} = -\frac{1}{2}\rho_0 w a(\theta)^{-3(1+w)}(\tau-\theta)^{-(\mu-1)(w+1)}. \tag{16}$$

Here, we have substituted the lapse function $N = 1$ after the variation.

To designate the temporary independent variables, the rule $(\tau, \theta) \mapsto (2t, t)$ is applied, where new cosmological time t [34] is used, where the dots denote these derivatives. Furthermore, the Hubble parameter is $H \equiv \dot{a}/a$. Hence, Equations (15) and (16) and the conservation Equation (13) can be written as

$$\dot{H}(t) + \frac{(1-\mu)H(t)}{t} + \frac{3H(t)^2}{2} + \frac{(\mu-2)(\mu-1)}{2t^2} = -\frac{1}{2}p(t), \tag{17}$$

$$H(t)^2 + \frac{(1-\mu)H(t)}{t} = \frac{1}{3}\rho(t), \tag{18}$$

$$\dot{\rho}(t) = -3\left(H(t) + \frac{(1-\mu)}{3t}\right)(p(t)+\rho(t)) \tag{19}$$

where expressions (11) and (12) are transformed to

$$\rho(t) = \rho_0\left[a(t)^{-3}t^{-(\mu-1)}\right]^{1+w}, \text{ and } p(t) = w\rho_0\left[a(t)^{-3}t^{-(\mu-1)}\right]^{1+w}, \tag{20}$$

which defines the energy density and the isotropic pressure of the matter fields in cosmological time.

2.4. Some Cosmological Solutions

From (18) and assuming $p = 0$ ($w = 0$), the Hubble parameter is

$$H(t) = \frac{\mu-1}{2t}\left[1 + \sqrt{1 + \frac{4}{3}\rho(t)\left(\frac{t}{\mu-1}\right)^2}\right]. \tag{21}$$

We have considered the positive root because we are interested in expanding universes.

To understand the self-accelerating behavior of H, let us assume that there is no matter, i.e., $\rho = 0$ and $\mu > 1$. Then, from (18),

$$H(t) = \frac{\mu-1}{t} \implies a(t) = \left(\frac{t}{t_0}\right)^{\mu-1}. \tag{22}$$

Henceforth,

$$H(t \to \infty) \to 0, \quad a(t \to \infty) \to \infty, \quad \text{if } \mu > 1 \tag{23}$$

and the deceleration parameter can be expressed as $1 + q = -\dot{H}/H^2$. Therefore,

$$q = -1 + \frac{1}{\mu - 1}, \tag{24}$$

and

$$\mu > 1 \implies q > -1, \tag{25}$$

where the usual case $q = -1$, corresponding to a cosmological constant Λ, is excluded.

The case $\rho = 0$ can also be interpreted as a fluid whose energy density quickly vanishes with evolution. The asymptotic solution (22) was examined in detail using a dynamical systems analysis in reference [61], and its properties are summarized in Table 1. The table summarizes the asymptotic behavior for $\mu > 1$ when the energy density of matter tends to zero. Hence, even in the absence of matter, fractional cosmology gives a power-law solution $a(t) = (t/t_0)^{\mu-1}$, which is accelerated for $\mu > 2$. This is a crucial difference to standard cosmology, where we must add a cosmological constant, quintessence scalar field, or other exotic fluids to accelerate the expansion.

Table 1. Asymptotic solution P_4, examined in reference [61].

Label	Ω_m	H	q	Acceleration?	Stability	Scale Factor
P_4	0	$\frac{\mu-1}{t}$	$-\frac{\mu-2}{\mu-1}$	Accelerated ($\mu > 2$)	Sink ($\mu > 2$)	Power law
				Decelerated ($1 < \mu < 2$)	Source ($\mu < 7/4$)	$a(t) = (t/t_0)^{\mu-1}$
					Saddle ($7/4 < \mu < 2$)	

Solving algebraically Equations (17)–(19) for $\dot{H}$, $\dot{\rho}$ and ρ, we obtain

$$\dot{H} = -\frac{1}{2}p + \frac{(\mu - 1)H}{t} - \frac{3}{2}H^2 - \frac{(\mu - 2)(\mu - 1)}{2t^2}, \tag{26}$$

$$\dot{\rho} = -\frac{3(\mu - 1)^2 H}{t^2} + \frac{12(\mu - 1)H^2}{t} - 9H^3 + p\left(\frac{\mu - 1}{t} - 3H\right), \tag{27}$$

$$\rho = 3H^2 - \frac{3(\mu - 1)H}{t}. \tag{28}$$

In General Relativity (GR), we have the flat Friedmann–Lemaître–Robertson–Walker metric; the main equations are the Friedmann constraint and conservation equation,

$$3H^2 = \rho, \tag{29}$$

$$\dot{\rho} + 3H(\rho + p) = 0. \tag{30}$$

Using (29) and (30), we obtain

$$2\dot{H} = -(\rho + p). \tag{31}$$

Now, using (29) and (31) we re-obtain (30). That is, we have three equations, two of them independent. However, as we discussed before, [62] studied Equations (17)–(19), and using a similar procedure as in GR, we obtain a new equation (see Equation (34)) instead of showing that two out of three equations are independent.

By demanding that (18) is conserved in time, i.e.,

$$\frac{d}{dt}\left[H(t)^2 + \frac{(1 - \mu)H(t)}{t} - \frac{1}{3}\rho(t)\right] = 0, \tag{32}$$

we calculate the corresponding derivatives and substitute them into (26)–(28) to obtain

$$\frac{(\mu - 1)(t(tp - 3H(tH + 2\mu - 6)) + 3(\mu - 2)(\mu - 1))}{6t^3} = 0. \tag{33}$$

This equation is an identity for $\mu = 1$ as expected in standard cosmology. However, for $\mu \neq 1$, we acquire the new relation for the pressure of the fluid:

$$p(t) = \frac{6(\mu - 3)H(t)}{t} + 3H^2(t) - \frac{3(\mu - 2)(\mu - 1)}{t^2}. \tag{34}$$

Using a similar procedure as in GR, we obtain a new Equation (34) instead of showing that two out of three equations are independent. This characteristic of fractional cosmology leads to some restrictions of the matter fields in the Universe that were explored in [62] for different matter fields.

Replacing the expression of p defined by (34) into (26) and (27), we obtain

$$\dot{H} = -\frac{2(\mu - 4)H}{t} - 3H^2 + \frac{(\mu - 2)(\mu - 1)}{t^2}, \tag{35}$$

$$\dot{\rho} = \frac{3(\mu - 1)(4\mu - 11)H}{t^2} - \frac{3(\mu - 13)H^2}{t} - 18H^3 - \frac{3(\mu - 2)(\mu - 1)^2}{t^3}. \tag{36}$$

The previous results are valid for any ideal gas source.

Moreover, following references [61,62], the system can be extended by including several matter sources in Equations (15) and (16). After performing algebra, and using $8\pi G = 1$, the following Raychaudhuri equation (with $N(t) = 1$) is obtained:

$$\dot{H} + \frac{(\mu - 1)H}{2t} + \frac{(\mu - 2)(\mu - 1)}{2t^2} = -\frac{1}{2}\sum_i (p_i + \rho_i), \tag{37}$$

along with the Friedmann equation

$$H^2 + \frac{(1 - \mu)}{t}H = \frac{1}{3}\sum_i \rho_i. \tag{38}$$

Furthermore, the continuity equation leads to

$$\sum_i \left[\dot{\rho}_i + 3\left(H + \frac{1 - \mu}{3t}\right)(\rho_i + p_i)\right] = 0, \tag{39}$$

where ρ_i and p_i are the density and pressure of the ith matter component, respectively, and the sum is over all species, e.g., matter, radiation, etc. Note that when $\mu = 1$ in Formula (38) and Formula (39), the standard cosmology without Λ is recovered, which by itself does not produce an accelerated expanding universe.

Using the equation of state $p_i = w_i \rho_i$, where $w_i \neq -1$ and are constants, we have

$$\sum_i (1 + w_i)\rho_i \left[\frac{\dot{\rho}_i}{(1 + w_i)\rho_i} + 3\frac{\dot{a}}{a} + \frac{1 - \mu}{t}\right] = \sum_i (1 + w_i)\rho_i \frac{d}{dt}\left[\ln\left(\rho_i^{1/(1+w_i)} a^3 t^{1-\mu}\right)\right]. \tag{40}$$

Assuming separate conservation equations for each species and integrating for each ρ_i, we have the following solution:

$$\rho_i(t) = \rho_{0i} a(t)^{-3(1+w_i)}(t/t_0)^{(\mu-1)(1+w_i)}, \tag{41}$$

where $a(t_0) = 1$, t_0 is the age of the universe and ρ_{0i} is the current value of the energy density of the ith species. Therefore, by substituting (41) into (38), we have

$$H^2 + \frac{(1-\mu)}{t} H = \frac{8\pi G}{3} \sum_i \rho_{0i} a^{-3(1+w_i)} (t/t_0)^{(\mu-1)(1+w_i)}. \tag{42}$$

Note that for $\mu \neq 1$, the modified continuity Equation (39) provides the condition

$$\frac{8\pi G}{3} \sum_i p_i = \frac{2(\mu-3)H}{t} + H^2 - \frac{(\mu-2)(\mu-1)}{t^2}. \tag{43}$$

Combining these results with (37) and (38), we have the Riccati equation (35). This equation generically appears in fractional cosmology, independent of the matter content. Therefore, in the following, we consider only one matter source.

Comparing with other fractional formulations, according to [42,44], and assuming $\Lambda = 0$ and using $8\pi G\Gamma(\mu) = 1$ for simplicity, we obtain the field equations

$$2\dot{H} + 3H^2 + 2\frac{(1-\mu)}{t}H + \frac{(1-\mu)(2-\mu)}{t^2} = -t^{1-\mu}P, \tag{44}$$

$$3H^2 + 3(1-\mu)\frac{H}{t} = t^{1-\mu}\varrho, \tag{45}$$

$$\dot{\varrho} + 3H(\varrho + P) = 0, \tag{46}$$

where ϱ and P are the bare dark matter energy density and pressure, respectively. Equations (44)–(46) are equivalent to (17)–(19) under the scaling

$$(\rho, p) = t^{1-\mu}(\varrho, P). \tag{47}$$

Now, we consider a constant EoS,

$$P = w\varrho. \tag{48}$$

Then, one obtains,

$$w = -1 + \frac{2}{3}\left[1 + q(t) - \frac{(\mu-1)}{2tH(t)} - \frac{(\mu-1)(\mu-2)}{2(tH(t))^2}\right]\left(1 - \frac{\mu-1}{tH(t)}\right)^{-1}. \tag{49}$$

Then, for $\mu = 1$ we have

$$3H^2 = \rho, \tag{50}$$

$$2\dot{H} + 3H^2 = -p \implies 2\dot{H} = -(\rho + p), \tag{51}$$

and

$$q = \frac{1}{2}\left[1 + 3\left(\frac{p}{\rho}\right)\right] = \frac{1}{2}(1 + 3w) \implies w = \frac{1}{3}(2q - 1). \tag{52}$$

Furthermore, we recover GR.

From Equations (45) and (44) and $\mu \neq 1$, it follows that

$$2\dot{H} - \frac{(1-\mu)}{t}H + \frac{(1-\mu)(2-\mu)}{t^2} = -t^{1-\mu}(1+w)\varrho. \tag{53}$$

Replacing (45), we recover (49).

Setting $w = 0$, from (49) we obtain

$$q(t) = \frac{1}{2} + \left(\frac{\mu - 1}{tH(t)}\right)\left(\frac{(\mu/2 - 1)}{tH(t)} - 1\right). \tag{54}$$

That is, a "correction" to the usual CDM ($\mu = 1$, $w = 0$, $q = 1/2$).
Using (54) and the relation $q = -1 - \dot{H}/H^2$, we obtain the equation for H as

$$\dot{H} = \frac{(\mu - 1)H}{t} - \frac{3}{2}H^2 - \frac{(\mu - 2)(\mu - 1)}{2t^2}. \tag{55}$$

For $\mu = 1$, we recover the usual CDM ($w = 0$, $q = 1/2$),

$$H(t) = \frac{2H_0}{3H_0(t - t_0) + 2}, \quad q = \frac{1}{2}. \tag{56}$$

For $\mu = 2$, the solution of (55) is

$$H(t) = \frac{4H_0 t}{3H_0(t - t_0)(t + t_0) + 4t_0}, \quad q(t) = \frac{1}{2} - \frac{1}{tH} = -\frac{1}{4} - \frac{t_0}{H_0 t^2} + \frac{3t_0^2}{4t^2}. \tag{57}$$

We will search for solutions considering relativistic matter/radiation. Setting $w = 1/3$, from (49), we obtain

$$q(t) = 1 + \frac{(\mu - 2)(\mu - 1)}{2t^2 H(t)^2} - \frac{3(\mu - 1)}{2tH(t)}. \tag{58}$$

Using (58) and the relation $q = -1 - \dot{H}/H^2$, we obtain the equation for H as

$$\dot{H} = \frac{3(\mu - 1)H}{2t} - 2H^2 - \frac{(\mu - 2)(\mu - 1)}{2t^2}. \tag{59}$$

For $\mu = 1$, we recover the usual radiation ($w = 1/3$, $q = 1$),

$$H(t) = \frac{H_0}{2H_0(t - t_0) + 1}, \quad q = 1. \tag{60}$$

For $\mu = 2$, the solution of (59) is

$$H(t) = \frac{5H_0 t^{3/2}}{4H_0\left(t^{5/2} - t_0^{5/2}\right) + 5t_0^{3/2}}, \tag{61}$$

and

$$q(t) = \frac{(\mu - 2)(\mu - 1)t_0^3(5 - 4H_0 t_0)^2}{50H_0^2 t^5} - \frac{(\mu - 1)(8\mu - 31)t_0^{3/2}(4H_0 t_0 - 5)}{50H_0 t^{5/2}}$$
$$+ \frac{1}{25}\left(8\mu^2 - 54\mu + 71\right). \tag{62}$$

Another case of interest is when $w = -1$ (quasi-vacuum matter, according to [42,44]). The equation for H becomes

$$\dot{H} = -\frac{(\mu - 1)H}{2t} - \frac{(\mu - 2)(\mu - 1)}{2t^2}. \tag{63}$$

The solution to $H(t)$ turns out to be

$$H(t) = H_0 \left(\frac{t}{t_0} \right)^{-\frac{\mu-1}{2}} + \frac{(\mu-2)(\mu-1)}{(3-\mu)t} \left[1 - \left(\frac{t}{t_0} \right)^{\frac{3-\mu}{2}} \right]. \tag{64}$$

According to (64),

$$q(t) = -1 + \left[\frac{H_0(\mu-1)\left(\frac{t}{t_0} \right)^{\frac{1}{2}-\frac{\mu}{2}}}{2t} - \frac{(\mu-2)(\mu-1)\left(1 - \left(\frac{t}{t_0} \right)^{\frac{3}{2}-\frac{\mu}{2}} \right)}{(\mu-3)t^2} \right.$$

$$\left. + \frac{(\mu-2)(\mu-1)\left(\frac{t}{t_0} \right)^{-\frac{\mu}{2}-\frac{1}{2}}}{2t_0^2} \right] H(t)^{-2}. \tag{65}$$

For $0 < \mu < 3$, we have

$$q(t \to \infty) \to -1. \tag{66}$$

Hence, we obtain a late-time de Sitter solution without including a cosmological constant.

In summary, fractional cosmology allows for an accelerated expansion without adding exotic fluids to the model. Therefore, we now consider a model with cold dark matter to present a specific realization of these possibilities.

2.5. Model with Cold Dark Matter

Assume

$$H(t) = \frac{\alpha}{t}, \tag{67}$$

where α is a constant and $\mu > 1$. If $\alpha = \mu - 1$, we recover Equation (22).

The conservation equation for matter (19), for cold dark matter ($p_{\text{CDM}} = w_{\text{CDM}}\rho_{\text{CDM}}$ and $w_{\text{DM}} = 0$), takes the form

$$\dot{\rho}_{\text{CDM}} + 3H \left(1 + \frac{1-\mu}{3Ht} \right) \rho_{\text{CDM}} = 0, \tag{68}$$

when then reduces to

$$\dot{\rho}_{\text{CDM}} + \frac{(3\alpha - \mu + 1)\rho_{\text{CDM}}}{t} = 0. \tag{69}$$

Hence, we have for the matter energy density,

$$\rho_{\text{CDM}} = \rho_{CDM(0)} (t/t_0)^{-3\alpha+\mu-1}. \tag{70}$$

Choosing

$$\alpha = \frac{\mu+1}{3}, \tag{71}$$

we obtain

$$\rho_{\text{CDM}} = \rho_{CDM(0)} (t/t_0)^{-2}. \tag{72}$$

Then, from Equation (28), we obtain

$$\rho_{CDM(0)} = \frac{2(2-\mu)(\mu+1)}{3t_0^2}. \tag{73}$$

Using the redshift parameter $1 + z = 1/a$, we obtain

$$H(t) = \frac{\alpha}{t} \implies a(t) = \left(\frac{t}{t_0} \right)^{\alpha}, \tag{74}$$

and

$$1 + z = \frac{1}{a} \implies \left(\frac{t}{t_0}\right) = (1+z)^{-\frac{1}{\alpha}}, \tag{75}$$

then,

$$\rho_{\text{CDM}}(z) = \rho_{\text{CDM}}(0)(1+z)^{\frac{2}{\alpha}} \text{ and } H(z) = H_0(1+z)^{\frac{1}{\alpha}}, \tag{76}$$

where α is defined by (71). Comparing with GR, where the EoS w_{eff} is defined through

$$\rho_{\text{CDM}}(z) = \rho_{\text{CDM}}(0)(1+z)^{3(1+w_{\text{eff}})}, \tag{77}$$

we have

$$w_{\text{eff}} = -1 + \frac{2}{3\alpha} = -1 + \frac{2}{\mu+1} \text{ and } q = -1 + \frac{1}{\alpha} = -1 + \frac{3}{\mu+1}. \tag{78}$$

Similarly to GR, we have the usual relation $q = \frac{1}{2}(1 + 3w_{\text{eff}})$. Therefore, in fractional cosmology, we have an acceleration ($\ddot{a} > 0, q < 0$) as is present in GR when the effective fluid has $w_{\text{eff}} < -1/3$. Hence,

$$\ddot{a}(t) < 0, q > 0, w_{\text{eff}} > -1/3 \iff 1 < \mu < 2, \tag{79}$$

and

$$\ddot{a}(t) > 0, q < 0, w_{\text{eff}} < -1/3 \iff \mu > 2. \tag{80}$$

Finally, we have an accelerated expansion if $\mu > 2$, caused by the fractional derivative correction and not by the matter content. That is the powerful advantage of fractional cosmology over GR. This is consistent as $\rho_{\text{CDM}} \to 0$ with the asymptotic solution $H(t) = \frac{\mu-1}{t}$, where $q = -\frac{\mu-2}{\mu-1}$, which is a power-law solution $a(t) = (t/t_0)^{\mu-1}$. It is accelerated if $\mu > 2$ and decelerated if $1 < \mu < 2$, as proven in [61].

2.6. Interpretation of the Fractional Term as a Dark Energy Source

We write (18) as

$$3H^2 = \rho_{\text{CDM}} + \rho_{\text{frac}}, \tag{81}$$

where

$$\rho_{\text{CDM}}(z) = \rho_{\text{CDM}}(0)(1+z)^{\frac{2}{\alpha}} = \frac{2(2-\mu)(\mu+1)}{3t_0^2}(1+z)^{\frac{6}{1+\mu}}, \tag{82}$$

where

$$\rho_{\text{frac}}(t) = \frac{3(\mu-1)}{t}H \underbrace{\implies}_{\text{using (67) and (75)}} \rho_{\text{frac}}(z) = \rho_{\text{frac}}(0)(1+z)^{\frac{2}{\alpha}}, \tag{83}$$

and

$$\rho_{\text{frac}}(0) = \frac{3(\mu-1)}{t_0}H_0 = \frac{(\mu-1)}{t_0 H_0}3H_0^2. \tag{84}$$

Using $H = d\ln a/dt$ and $1 + z = 1/a$, we obtain

$$t_0 H_0 = \int_0^\infty \frac{dz}{(1+z)E(z)}. \tag{85}$$

Substituting (see Equation (67))

$$E(z) = (1+z)^{\frac{1}{\alpha}} = (1+z)^{\frac{3}{1+\mu}}, \tag{86}$$

with α defined by (71), we obtain

$$H_0 t_0 = (1 + \mu)/3. \tag{87}$$

On the other hand, using (81), (83) and (84), we obtain

$$E^2(z) = \frac{3H^2(z)}{3H_0^2} = \frac{\rho_{\text{CDM}}(z)}{3H_0^2} + \frac{\rho_{\text{frac}}(z)}{3H_0^2} \iff E^2(z) = \Omega_{\text{DM}}(z) + \Omega_{\text{frac}}(z), \tag{88}$$

$$\implies \Omega_{\text{frac}}(0) = 1 - \Omega_{\text{DM}}(0) = \frac{\mu - 1}{t_0 H_0} = \frac{3(\mu - 1)}{\mu + 1} \sim 0.744\%, \ \mu \sim 1.65957, \tag{89}$$

where $\Omega_{\text{DM}}(0) \sim 0.256\%$. Compare the value $\mu \sim 1.66$, with the observational tests performed in [61] for a flat prior $1 < \mu < 3$, where the best-fit value for μ is $\mu^* = 1.71$.

We inspect more the nature of ρ_{frac} as an effective fluid in GR, i.e.,

$$\rho_{\text{frac}} = \frac{3(\mu - 1)}{t} H, \ q = -1 - \frac{\dot{H}}{H^2} \implies \dot{\rho}_{\text{frac}} = -H \left(1 + q + \frac{1}{Ht} \right) \rho_{\text{frac}}, \tag{90}$$

$$\implies \dot{\rho}_{\text{frac}} + 3H(1 + w_{\text{frac}}) \rho_{\text{frac}} = 0, \tag{91}$$

where $w_{\text{frac}} = \frac{1}{3} \left(q - 2 + \frac{1}{\alpha} \right)$. According to (78), we deduce again (77),

$$w_{\text{frac}} = -1 + \frac{2}{3\alpha}, \tag{92}$$

corresponding to quintessence $(-1 < w_{\text{frac}} < -1/3)$ if $\mu > 2$.

3. Exact Solutions

3.1. First Exact Solution

From Equations (28) and (34) and defining the effective equation of state $w := p/\rho$, we have

$$w = \frac{\mu - 2}{tH} + \frac{2\mu - 5}{tH - \mu + 1}. \tag{93}$$

Assuming $w \neq -1$ and is a constant, and by solving (93) algebraically for H, we obtain

$$H_{1,2}(t) = \frac{\alpha_\pm}{t}, \tag{94}$$

$$\alpha_\pm = -\frac{6 - 2\mu + (1 - \mu)w \pm \sqrt{\mu^2(w^2 + 8) + w^2 - 2\mu(w(w + 2) + 18) + 4w + 44}}{2(w - 1)}. \tag{95}$$

Hence, in the intervals $-1 < w < 1, 1 < \mu < 2$, both $H_{1,2}(t)$ are non-negative. For $-1 < w < 1, \mu > 2$, $H_1(t)$ is negative and $H_2(t)$ is positive. For $\mu \in \{1, 2\}$, $H_1(t)$ is zero.

The deceleration parameter for each algebraic solution is a constant

$$q_{1,2}(t) := -1 - \dot{H}_{1,2}(t)/H_{1,2}^2(t) = -1 + 1/\alpha_\pm, \tag{96}$$

such that the solutions for the scale factor are power laws.

Therefore, upon physical consideration, we select the one that gives an accelerated Universe. The deceleration parameter $q_1(t)$ is negative in the parameter region $-1 < w < 1, 1 < \mu < 2$, and we have an accelerated expansion when $H(t) = H_1(t)$ and $(\mu, w) \in [-1, 1] \times [1, 2]$. If we choose the range $-1 < w < 1, 2 < \mu < 3$, the solution $H_1(t)$ becomes nonphysical, and the one that gives accelerated expansion is $H_2(t)$ because $q_2(t)$ is negative in the parameter region $-1 < w < 1, 2 < \mu < 3$.

Substituting (94), (28) and (34) into (26) and (27), we obtain the compatibility conditions

$$-2\alpha_{\pm}\mu - 3(\alpha_{\pm} - 3)\alpha_{\pm} + \mu^2 - 3\mu + 2 = 0, \tag{97}$$

$$(2\alpha_{\pm} - \mu + 1)\left(2\alpha_{\pm}\mu + 3(\alpha_{\pm} - 3)\alpha_{\pm} - \mu^2 + 3\mu - 2\right) = 0, \tag{98}$$

where $\alpha_{\pm}$ is defined by (95) for the existence of an exact solution. We define the current value of $H(t_0) = H_0$ through $H_0 t_0 = \alpha_{\pm}$, and $\alpha_{\pm}$ is interpreted as the age parameter $\alpha = tH$ evaluated at t_0 (the current time).

Therefore, to obtain solutions, we solve (97) and (98) simultaneously for μ and w. Upon physical consideration, we remove the cases with $w = -1$ and $\mu \in \{1, 2\}$, and we assume $-1 < w < 1$.

From (94), the definition of q and Equations (28), (34) and (93), we have

$$a(t) = \left(\frac{t}{t_0}\right)^{\alpha_{\pm}}, \quad H(t) = \frac{\alpha_{\pm}}{t}, \quad q(t) = -1 + \frac{1}{\alpha_{\pm}},$$

$$p(t) = \frac{3\left(\alpha_{\pm}^2 + 2\alpha_{\pm}(\mu - 3) - (\mu - 2)(\mu - 1)\right)}{t^2}, \quad \rho(t) = \frac{3\alpha_{\pm}(1 - \mu + \alpha_{\pm})}{t^2},$$

and

$$w := p(t)/\rho(t) = \frac{\mu}{\alpha_{\pm}} + \frac{2\alpha_{\pm} - 3}{1 - \mu + \alpha_{\pm}} - \frac{\alpha_{\pm} + 2}{\alpha_{\pm}}, \tag{99}$$

where we set the conditions $a'(t_0) = H_0$, and fix the current value of the scale factor to $a(t_0) = 1$.

For simplicity, let us assume that the source is dust, with $p = 0$ ($w = 0$). Then, we have $\alpha_{\pm} = 3 - \mu + \epsilon\sqrt{\mu(2\mu - 9) + 11}$, where $\epsilon = \pm 1$, which makes (99) an identity.

Hence, we have

$$H_{1,2}(t) = \frac{3 - \mu + \epsilon\sqrt{\mu(2\mu - 9) + 11}}{t}, \tag{100}$$

$$\rho(t) = \frac{3\left(\mu - \epsilon\sqrt{\mu(2\mu - 9) + 11} - 3\right)\left(2\mu - \epsilon\sqrt{\mu(2\mu - 9) + 11} - 4\right)}{t^2}. \tag{101}$$

Substituting in (26) and (27), we obtain the compatibility conditions (replace $w = 0$ in (97) and (98)),

$$-3(\mu(2\mu - 9) + 11) + \sqrt{\mu(2\mu - 9) + 11}(4\mu - 9)\epsilon + 2 = 0, \tag{102}$$

$$-(17\mu - 39)(\mu(2\mu - 9) + 11) + 6\mu + 6(\mu(2\mu - 9) + 11)^{3/2}\epsilon$$

$$+ (\mu(12\mu - 55) + 59)\sqrt{\mu(2\mu - 9) + 11}\epsilon - 14 = 0. \tag{103}$$

For $\epsilon = -1$, the two conditions are simultaneously satisfied only for $\mu \in \{1, 2\}$.

For $\epsilon = 1$, the two conditions are simultaneously satisfied only for $\mu \in \{5/2, 7/2\}$. Since we are interested in the case where $\mu \notin \{1, 2\}$ and an expanding Universe ($H > 0$), the parameter that gives the physical solution $H(t) = H_2(t)$ is $\mu = 5/2$. Substituting these values for w and μ, we obtain

$$(p(t), \rho(t), H(t)) \rightarrow \left(0, 0, \frac{3}{2t}\right) \implies a(t) = a_0 t^{3/2}. \tag{104}$$

That means if we fix the equation of state w, there are specific values that μ has to satisfy to obtain an exact solution.

3.2. Second Exact Solution

One can also solve a Riccati equation for $\mu \neq 1$:

$$\dot{H}(t) = \frac{(\mu - 1)(3w + 2)H(t)}{2t} - \frac{3}{2}(w + 1)H(t)^2 - \frac{(\mu - 2)(\mu - 1)}{2t^2} \tag{105}$$

which follows from substituting $p = w\rho$ into (26) and removing ρ using (28). We obtain the exact solution

$$H(t) = \frac{1}{3t(w + 1)}\left[\mu + \beta + \frac{3}{2}(\mu - 1)w - \frac{2b_1 t_0^\beta \beta}{t^\beta + b_1 t_0^\beta}\right], \tag{106}$$

where

$$b_1 = \frac{2(\beta + \mu) - 6H_0 t_0(w + 1) + 3(\mu - 1)w}{2\beta + 6H_0 t_0(w + 1) - 2\mu - 3\mu w + 3w} \tag{107}$$

is an integration constant, H_0 is the current value of H at $t = t_0$ and

$$\beta = \frac{1}{2}\sqrt{-4(\mu(2\mu - 9) + 6) + 9(\mu - 1)^2 w^2 + 24(\mu - 1)w}. \tag{108}$$

Substituting in (26) and (27), we obtain the compatibility conditions

$$-4\beta(\beta - 4\mu + 9) + \frac{8\beta^2(w - 1)t^{2\beta}}{\left(t^\beta + b_1 t_0^\beta\right)^2} - 3(\mu - 1)(3\mu - 13)w^2 + w\left(4\beta(5\mu - 12) - 8\mu^2 + 42\mu - 6\right) + 24$$

$$- \frac{8\beta t^\beta(-\beta + 4\mu + w(\beta + 5\mu - 12) - 9)}{t^\beta + b_1 t_0^\beta} = 0, \tag{109}$$

$$t^{2\beta}\left(4\beta(\beta + 4\mu - 9) + 3(\mu - 1)(3\mu - 13)w^2 + w\left(4\beta(5\mu - 12) + 8\mu^2 - 42\mu + 6\right) - 24\right)$$

$$+ 2b_1 t^\beta t_0^\beta\left(w\left(4\beta^2 + \mu^2(9w + 8) - 6\mu(8w + 7) + 39w + 6\right) - 24\right)$$

$$+ b_1^2 t_0^{2\beta}\left(4\beta(\beta - 4\mu + 9) + 3(\mu - 1)(3\mu - 13)w^2 + w\left(\beta(48 - 20\mu) + 8\mu^2 - 42\mu + 6\right) - 24\right) = 0. \tag{110}$$

These compatibility conditions have to be satisfied for all t, such that $b_1 = 0$. Then, (106) becomes

$$H(t) = \frac{1}{3t(w + 1)}\left[\mu + \beta + \frac{3}{2}(\mu - 1)w\right], \tag{111}$$

and the compatibility conditions are

$$-4\beta(\beta + 4\mu - 9) - 3(\mu - 1)(3\mu - 13)w^2 + w\left(\beta(48 - 20\mu) - 8\mu^2 + 42\mu - 6\right) + 24 = 0, \tag{112}$$

$$4\beta(\beta + 4\mu - 9) + 3(\mu - 1)(3\mu - 13)w^2 + w\left(4\beta(5\mu - 12) + 8\mu^2 - 42\mu + 6\right) - 24 = 0. \tag{113}$$

Therefore, to obtain solutions, we solve (112) and (113) simultaneously for μ and w. Upon physical consideration, we remove the cases with $w = -1$ and $\mu \in \{1, 2\}$, and we assume $-1 < w < 1$.

As before, we choose dust matter ($p = 0, w = 0$). Then,

$$H(t) = \frac{\mu + \sqrt{(9 - 2\mu)\mu - 6}\left(1 - \frac{2b_1}{b_1 + t^{\sqrt{(9 - 2\mu)\mu - 6}}}\right)}{3t}. \tag{114}$$

As before, two compatibility conditions are satisfied only for $b_1 = 0$ and $\mu \in \{5/2, 7/2\}$.

For $b_1 = 0$ and $\mu = 5/2$, we have the physical solution

$$(p(t), \rho(t), H(t)) \to \left(0, 0, \frac{3}{2t}\right) \implies a(t) = a_0 t^{3/2}. \tag{115}$$

For $b_1 = 0$ and $\mu = 7/2$, we have the nonphysical solution

$$(p(t), \rho(t), H(t)) \to \left(0, -\frac{9}{2t^2}, \frac{3}{2t}\right). \tag{116}$$

As in the previous section, if we impose the equation of the state of the fluid as dust, this fixes the values of μ to $5/2$.

3.3. General Solution

In this section, we are interested in an exact solution that gives the general solution of the system. For this purpose, one can solve the Riccati Equation (35) independent of the EoS. That has the $H(t)$ solution defined by

$$H(t) = \frac{1}{3t}\left[\frac{9 - 2\mu + r}{2} - \frac{cr\alpha_0^r}{c\alpha_0^r + (H_0 t)^r}\right], \tag{117}$$

where

$$c = \frac{-2\mu + r - 6\alpha_0 + 9}{2\mu + r + 6\alpha_0 - 9}, \text{ and } r = \sqrt{8\mu(2\mu - 9) + 105}, \tag{118}$$

and for the current time $\alpha_0 = H_0 t_0$, where t_0 is the value of t today. H_0 is the current value of the Hubble factor, α_0, for which we obtain the best-fit values.

That is the exact solution for $H(t)$ studied in [62] (see an analogous case in [36], Equation (36), and in [61], Equation (24)). In this case, expressions (28) and (34) are used to calculate $\rho(t)$ and $p(t)$. Substituting all the expressions in the system (26)–(28) leads to identities. There is an arbitrary constant of integration and the equations are identically satisfied (no compatibility equations are required); thus, this is the general solution of the system. This result is generic since it does not require specifying the EoS. Hence, Equation (117) gives a one-parameter family of solutions that gives a complete solution and is independent of the matter content.

Defining the dimensionless time variable $\tau = H_0 t$ such that $\alpha_0 = H_0 t_0$ and $\xi = \tau/\alpha_0 = t/t_0$, by definition, the current value of ξ is $\xi_0 = 1$ and the expressions become

$$a(\xi) = \xi^{\frac{1}{6}(-2\mu - r + 9)} \sqrt[3]{\frac{c + \xi^r}{(c+1)}}, \tag{119}$$

$$z(\xi) = -1 + \xi^{\frac{1}{6}(2\mu + r - 9)} \sqrt[3]{\frac{(c+1)}{c + \xi^r}}, \tag{120}$$

$$E(\xi) = \frac{H(\xi)}{H_0} = \frac{1}{3\alpha_0 \xi}\left[\frac{9 - 2\mu + r}{2} - \frac{cr}{c + \xi^r}\right], \tag{121}$$

$$p(\xi) = \frac{H_0^2\left(2(4\mu - 9)r(\xi^{2r} - c^2) + r^2(\xi^r - c)^2 - 7(4\mu(2\mu - 9) + 45)(c + \xi^r)^2\right)}{12\alpha_0^2 \xi^2 (c + \xi^r)^2}, \tag{122}$$

$$\rho(\xi) = \frac{H_0^2\left(-2(5\mu - 12)r(\xi^{2r} - c^2) + r^2(\xi^r - c)^2 + (2\mu - 9)(8\mu - 15)(c + \xi^r)^2\right)}{12\alpha_0^2 \xi^2 (c + \xi^r)^2}, \tag{123}$$

$$q(\xi) = -\frac{c^2(2\mu + r - 9)(2\mu + r - 3) + 2c(4\mu^2 - 24\mu + 5r^2 + 27)\xi^r + (-2\mu + r + 3)(-2\mu + r + 9)\xi^{2r}}{((-2\mu + r + 9)\xi^r - c(2\mu + r - 9))^2}, \tag{124}$$

$$w_{\text{eff}}(\xi) = \frac{2(4\mu - 9)r(\xi^{2r} - c^2) + r^2(\xi^r - c)^2 - 7(4\mu(2\mu - 9) + 45)(c + \xi^r)^2}{((-2\mu + r + 9)\xi^r - c(2\mu + r - 9))((-8\mu + r + 15)\xi^r - c(8\mu + r - 15))}, \tag{125}$$

$$\Omega_{\text{m}}(\xi) = \frac{(-8\mu + r + 15)\xi^r - c(8\mu + r - 15)}{(-2\mu + r + 9)\xi^r - c(2\mu + r - 9)}. \tag{126}$$

Taking the limit $\xi \to \infty$, we have

$$\lim_{\xi \to \infty} z(\xi) = -1, \quad \lim_{\xi \to \infty} a(\xi) = \infty, \quad \lim_{\xi \to \infty} E(\xi) = 0, \quad \lim_{\xi \to \infty} p(\xi) = 0, \quad \lim_{\xi \to \infty} \rho(\xi) = 0,$$

$$\lim_{\xi \to \infty} q(\xi) = \frac{-13 - 2(\mu - 4)\mu + \sqrt{8\mu(2\mu - 9) + 105}}{2(\mu - 2)(\mu - 1)},$$

$$\lim_{\xi \to \infty} w_{\text{eff}}(\xi) = \frac{-7 + \sqrt{8\mu(2\mu - 9) + 105}}{4(\mu - 1)}, \quad \lim_{\xi \to \infty} \Omega_{\text{m}}(\xi) = \frac{5 - \sqrt{8\mu(2\mu - 9) + 105}}{2(\mu - 2)},$$

and

$$\lim_{\xi \to \infty} \alpha(\xi) = \frac{1}{6}\left(9 - 2\mu + \sqrt{8\mu(2\mu - 9) + 105}\right) \geq 0, \tag{127}$$

where $\alpha(t) = tH$ is the age parameter.

The main difficulty of this approach is the need to invert (120) to obtain ξ as a function of z because the data are in terms of redshift, which is impossible using analytical tools. After all, the equation is a rational one. However, the variable ξ can be used as a parameter instead of z in the parametric representation.

3.4. Asymptotic Analysis

The following is a precise scheme which does not require inverting (120).

By introducing the logarithmic independent variable $s = -\ln(1 + z)$, with $s \to -\infty$ as $z \to \infty$, $s \to 0$ as $z \to 0$ and $s \to \infty$ as $z \to -1$, and defining the age parameter as $\alpha = tH$, we obtain the initial value problem

$$\alpha'(s) = 9 - 2\mu - 3\alpha(s) + \frac{(\mu - 2)(\mu - 1)}{\alpha(s)}, \tag{128}$$

$$t'(s) = t(s)/\alpha(s), \tag{129}$$

$$\alpha(0) = t_0 H_0, t(0) = t_0. \tag{130}$$

Equation (128) gives a one-dimensional dynamical system. The equilibrium points are $T_1 : \alpha = \frac{1}{6}\left(9 - 2\mu - \sqrt{8\mu(2\mu - 9) + 105}\right)$, that satisfies $\alpha > 0$ for $1 < \mu < 2$, and $T_2 : \alpha = \frac{1}{6}\left(9 - 2\mu + \sqrt{8\mu(2\mu - 9) + 105}\right)$, that satisfies $\alpha > 0$ for $\mu \in \mathbb{R}$.

The eigenvalue of T_1 is $-3 - 36(\mu - 2)(\mu - 1)\Big/\left(2\mu + \sqrt{8\mu(2\mu - 9) + 105} - 9\right)^2 > 0$ for $1 < \mu < 2$. Hence, T_1 is a source whenever it exists.

The eigenvalue of T_2 is $-3 - 36(\mu - 2)(\mu - 1)\Big/\left(-2\mu + \sqrt{8\mu(2\mu - 9) + 105} + 9\right)^2 < 0$ for $\mu \in \mathbb{R}$. Hence, T_2 is always a sink. It has asymptotic behavior for large s, which is consistent with [62], in which the attractor solution has an asymptotic age parameter

$$\lim_{t \to \infty} tH = \frac{1}{6}(9 - 2\mu + r). \tag{131}$$

We introduce the parameter ϵ_0 such that

$$\epsilon_0 = \frac{1}{2}\lim_{t\to\infty}\left(\frac{t_0 H_0 - tH}{tH}\right), \quad \alpha_0 = \frac{1}{6}\left(9 - 2\mu + \sqrt{8\mu(2\mu - 9) + 105}\right)(1 + 2\epsilon_0), \quad (132)$$

where ϵ_0 is a measure of the limiting value of the relative error in the age parameter tH when it is approximated by $t_0 H_0$. When $\epsilon_0 = 0$, $\alpha_0 = \frac{1}{6}(-2\mu + r + 9)$, which implies $c = 0$ in (120) and (121). Thus, we obtain the leading term

$$E(z) = (1 + z)^{\frac{6}{(9 - 2\mu + r)}}. \quad (133)$$

We obtain the exact value of $E(z)$ by integrating the initial value problem numerically

$$E'(z) = \frac{E(z)\tau(z)(3E(z)\tau(z) + 2\mu - 8) - (\mu - 2)(\mu - 1)}{(z + 1)E(z)\tau(z)^2}, \quad E(0) = 1, \quad (134)$$

$$\tau'(z) = -\frac{1}{(1 + z)E(z)}, \quad \tau(0) = \frac{1}{6}(2\epsilon_0 + 1)(9 - 2\mu + r). \quad (135)$$

3.5. Approximated Analytical Solution

Substituting $\alpha = e^{-3s}y^{\frac{1}{2}}$ into (128), it is transformed into the following equation:

$$\frac{dy}{ds} = 2(\mu - 2)(\mu - 1)e^{6s} + 2(9 - 2\mu)e^{3s}y^{\frac{1}{2}}. \quad (136)$$

Let m be the solution of the following Bernoulli equation

$$\frac{dm}{ds} = 2(9 - 2\mu)e^{3s}m^{\frac{1}{2}}. \quad (137)$$

The solutions of Bernoulli's Equation (137) are three:

$$m(s) = \begin{cases} 0 & \text{such that } m(0) = 0 \\ \frac{1}{9}\left[(9 - 2\mu)(1 - e^{3s}) - 3m_0^{\frac{1}{2}}\right]^2 & \text{such that } m(0) = m_0 \\ \frac{1}{9}\left[(9 - 2\mu)(1 - e^{3s}) + 3m_0^{\frac{1}{2}}\right]^2 & \text{such that } m(0) = m_0 \end{cases}. \quad (138)$$

Taking the difference term by term of (136) and (137), we obtain

$$\frac{dy}{ds} - \frac{dm}{ds} = 2(\mu - 2)(\mu - 1)e^{6s} + 2(9 - 2\mu)e^{3s}\left[y^{\frac{1}{2}} - m^{\frac{1}{2}}\right]. \quad (139)$$

Assuming $y = m + n$, where $n \geq 0$ is the remainder in the approximation of y by m, and considering the following inequality

$$(m + n)^{\frac{1}{2}} \leq m^{\frac{1}{2}} + n^{\frac{1}{2}} \quad (140)$$

for $m \geq 0$ and $n \geq 0$, from (139), we then obtain the differential inequality

$$\frac{dn}{ds} \leq 2(\mu - 2)(\mu - 1)e^{6s} + 2(9 - 2\mu)e^{3s}n^{\frac{1}{2}}. \quad (141)$$

Suppose that $n = A^2 e^{6s}$, where A is to be determined. Then, Equation (141) leads to

$$3A^2 \leq (\mu - 2)(\mu - 1) + (9 - 2\mu)A. \quad (142)$$

The equality occurs at A values of

$$A_- = \frac{1}{6}\left(9 - 2\mu - \sqrt{8\mu(2\mu - 9) + 105}\right), A_+ = \frac{1}{6}\left(9 - 2\mu + \sqrt{8\mu(2\mu - 9) + 105}\right), \quad (143)$$

which are the α values of the equilibrium points T_1 and T_2 of the one-dimensional dynamical system (128).

We choose the third solution of Bernoulli's equation in (138). Hence, we obtain an approximation of y, given by

$$y_{\text{approx}} = \frac{1}{9}\left[(9 - 2\mu)(1 - e^{3s}) + 3m_0^{\frac{1}{2}}\right]^2 + A^2 e^{6s}. \quad (144)$$

Then, we obtain an approximation of α, given by

$$\alpha_{\text{approx}}(s) = \left[\frac{1}{9}\left((9 - 2\mu)(1 - e^{3s}) + 3m_0^{\frac{1}{2}}\right)^2 e^{-6s} + A^2\right]^{\frac{1}{2}}. \quad (145)$$

Calculating the limit

$$\lim_{s \to +\infty} \alpha_{\text{approx}}(s) = \frac{1}{3}\sqrt{9A^2 + (9 - 2\mu)^2}, \quad (146)$$

and imposing the equality with (131), we have

$$A^2 = \frac{1}{9}\mu\left(\mu - \sqrt{8\mu(2\mu - 9) + 105} + 9\right) + \frac{1}{2}\sqrt{8\mu(2\mu - 9) + 105} - \frac{23}{6}, \quad (147)$$

which is non-negative and satisfies inequality (142) for $2 \le \mu \le \frac{1}{10}\left(63 + \sqrt{849}\right) \lesssim 9.21376$. Moreover, $A \in [0, A_+]$ for $2 \le \mu \le 3.25162$ or $7.59791 \le \mu \le 9.21376$.

To calculate m_0, we use the condition $\alpha_{\text{approx}}(0) = \alpha_0 := t_0 H_0$. Hence, $m_0 = \alpha_0^2 - A^2$. In terms of redshift, we have

$$\alpha_{\text{approx}}(z) = \left[\frac{1}{9}\left((9 - 2\mu)\left(1 - (1 + z)^{-3}\right) + 3\left(\alpha_0^2 - A^2\right)^{\frac{1}{2}}\right)^2 (1 + z)^6 + A^2\right]^{\frac{1}{2}}, \quad (148)$$

where A is defined by (147).

For Equation (129), we obtain

$$t^{-1}\frac{dt}{ds} = \left[\frac{1}{9}\left((9 - 2\mu)(1 - e^{3s}) + 3m_0^{\frac{1}{2}}\right)^2 e^{-6s} + A^2\right]^{-\frac{1}{2}}, \quad (149)$$

with the solution given by

$$t(s) = t_0 \exp\left(\int_0^s \left[\frac{1}{9}\left((9 - 2\mu)(1 - e^{3\zeta}) + 3m_0^{\frac{1}{2}}\right)^2 e^{-6\zeta} + A^2\right]^{-\frac{1}{2}} d\zeta\right). \quad (150)$$

Now, considering an asymptotic expansion of the integral for large values of s, where $m_0 = \alpha_0^2 - A^2$ and A is defined by (147), we obtain

$$t(s) \simeq t_0 e^{\int_0^s \frac{3}{\sqrt{9A^2 + (9 - 2\mu)^2}} d\zeta} = t_0 e^{\frac{3s}{\sqrt{9A^2 + (9 - 2\mu)^2}}}. \quad (151)$$

Consequently,

$$H(s) \simeq \frac{H_0}{\alpha_0}\left[\frac{1}{9}\left((9-2\mu)(1-e^{3s})+3m_0^{\frac{1}{2}}\right)^2 e^{-6s}+A^2\right]^{\frac{1}{2}} e^{-\frac{3s}{\sqrt{9A^2+(9-2\mu)^2}}}. \tag{152}$$

We have substituted an asymptotic expansion of the integral for large s given by (151). Finally,

$$E(z)=\frac{H(z)}{H_0}\simeq E_{\text{approx}}(z)$$

$$=\frac{1}{\alpha_0}\left[\frac{1}{9}\left((9-2\mu)\left(1-(1+z)^{-3}\right)+3m_0^{\frac{1}{2}}\right)^2(1+z)^6+A^2\right]^{\frac{1}{2}}(1+z)^{\frac{3}{\sqrt{9A^2+(9-2\mu)^2}}} \tag{153}$$

and

$$t(z)\simeq t_{\text{approx}}(z)=t_0(1+z)^{-\frac{3}{\sqrt{9A^2+(9-2\mu)^2}}}, \tag{154}$$

as $z \to -1$, where α_0 is defined by (132), A is defined by (147) and $m_0=\alpha_0^2-A^2$.

Figure 1 presents Expression (153) compared to the numerical solutions of (134) and (135), leading term $(1+z)^{\frac{6}{(9-2\mu+r)}}$ and $E(z)$ of ΛCDM for $\mu=2.5$ and different values of ϵ_0. The figure shows that generically, for $2\leq\mu\lesssim9.21376$, there is a good accuracy of the approximation of the exact value $E(z)$ by the asymptotic approximation (153) as $z\to-1$.
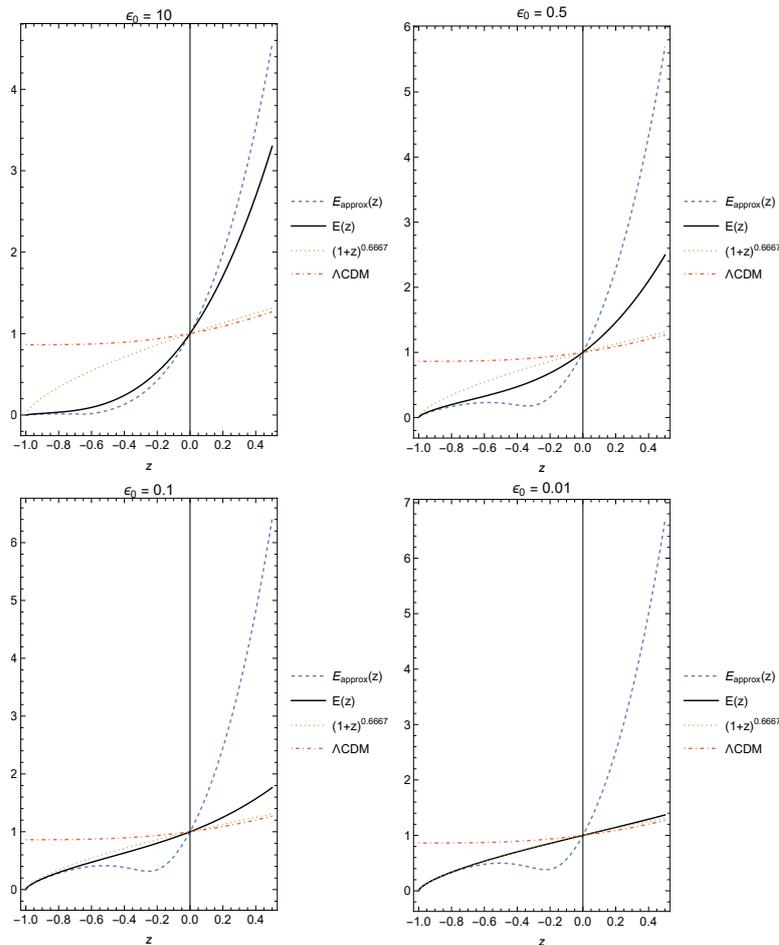
Figure 1. Expression (153) compared the numerical solution of (134) and (135), the leading term $(1+z)^{\frac{6}{(9-2\mu+r)}}$, $E(z)$ (ΛCDM) for $\mu=2.5$ and different values of ϵ_0.

3.6. Discussion

Our analysis shows differences between standard ΛCDM cosmology-based GR and the fractional version. Given the energy density expression ρ in GR, one can calculate the Hubble parameter through the Friedmann equation. Therefore, we deduce H and we investigate the cosmological history. Finally, we consider the existence of dark matter ($w = 0$), as $w = -1$ for Λ and $-1 < w < -1/3$ for quintessence, as suggested from the observations.

If we proceed as before, to give w, we use $w = p/\rho$ and then use the equations for ρ and p, i.e., Equations (28) and (34). With these expressions, one can calculate $H(t)$ and $q(t)$. In fractional cosmology, the asymptotic behavior $H(t) \sim 1/t$ is a characteristic due to the fractional parameter $\mu > 1$.

We related the possible matter scenarios, and according to the relevant discussion on the EoS w, we have two regimes of interest.

First, consider ρ-like dark matter with the behavior of dark energy, $-1 < w < -1/3$, i.e., quintessence. This case was investigated and the relevant results are summarized in the following.

In the first approach, we solve (93) for H, obtaining two solutions $H_{1,2}(t) = \frac{\alpha_\pm}{t}$, where the α parameter is defined by (95) and takes the values $\alpha_\pm$.

Therefore, to obtain solutions, we solved (97) and (98) simultaneously for μ and w. For $\epsilon = -1$, we have the following solutions for Equations (97) and (98):

- $w = \frac{7+\sqrt{8\mu(2\mu-9)+105}}{4(1-\mu)}$ if $\mu < 1$ or $1 < \mu < 2$ or $2 < \mu < \frac{5}{2}$ or $\mu > \frac{5}{2}$.
- $\mu = 1$ if $w \neq 1$.
- $\mu = 2$ if $1 < w \leq 2$ or $w < 1$.
- $\mu = \frac{5}{2}$ if $w \geq \frac{4}{3}$.
- $\mu = \frac{5}{2}$ if $w = -2$.

In this case, the equation of state for radiation is not recovered.

For $\epsilon = 1$, Equations (97) and (98) lead to

- $w = \frac{-7+\sqrt{8\mu(2\mu-9)+105}}{4(\mu-1)}$ if $\mu < 1$ or $1 < \mu < 2$ or $2 < \mu < \frac{5}{2}$ or $\mu > \frac{5}{2}$. In this case, the equation of state for radiation is recovered for $\mu = 41/8$.
- $\mu = 2$ if $w \geq 2$.
- $\mu = \frac{5}{2}$ if $1 < w \leq \frac{4}{3}$ or $w < 1$.
- $\mu = 1$ if $w = -\frac{5}{7}$.
- $\mu = 2$ if $w = -\frac{1}{2}$.

The second approach consisted of solving the Riccati equation (105) for $\mu \neq 1$ following substitution of $p = w\rho$ in (26) and removing ρ using (28). The exact solution is (106), where H_0 is the current value of H at $t = t_0$. From (26) and (27), we found that compatibility conditions have to be satisfied for all t. It is necessary that $b_1 = 0$. Therefore, to obtain solutions, we solved (112) and (113) simultaneously for μ and w. We have the following solutions:

- $w = -1$ if $\mu \geq 3$.
- $w = \frac{7+\sqrt{8\mu(2\mu-9)+105}}{4(1-\mu)}$ if $2 < \mu < \frac{5}{2}$ or $\mu > \frac{5}{2}$ or $\mu < 2$.
- $w = \frac{-7+\sqrt{8\mu(2\mu-9)+105}}{4(\mu-1)}$ if $2 < \mu < \frac{5}{2}$ or $\frac{5}{2} < \mu \leq \frac{1}{4}\left(9 + \sqrt{201}\right)$ or $\mu < 2$.
- $\mu = 2$ if $w \leq -\frac{4}{3}$.
- $\mu = \frac{5}{2}$ if $w \geq -\frac{8}{9}$.
- $\mu = 1$ if $w = -\frac{5}{7}$.
- $\mu = 2$ if $w = -\frac{1}{2}$.
- $\mu = \frac{5}{2}$ if $w = -2$.

Upon physical consideration, we remove the cases with $w = -1$ and $\mu \in \{1, 2\}$ and we assume $-1 < w < 1$.

Using the two previous approaches, one obtains power-law solutions of the type $a = (t/t_0)^\alpha$. Additionally, one has to impose two compatibility conditions which allow particular solutions to (μ, w). That means that any solution of the power law type is indeed a particular exact solution of the system, but not the general solution. To obtain an exact solution that gives the general solution of the system (for any value of the free parameters that have an integration constant), we solved the Riccati Equation (35) independent of the EoS. This gave us solution (117). This result is generic since it does not require specifying the EoS. That led to $a(\tau)$ given by (119), $H(\tau)$ given by (121), $p(\tau)$ given by (122), $\rho(\tau)$ given by (123), $q(\tau)$ given by (124), $w_{\text{eff}}(\tau)$ given by (125) and $\Omega_{\text{m}}(\tau)$ given by (126), where we defined the new time variable $\tau = H_0 t$, such that $\alpha_0 = H_0 t_0$, $c = \frac{-2\mu + r - 6\alpha_0 + 9}{2\mu + r + 6\alpha_0 - 9}$, and $r = \sqrt{8\mu(2\mu - 9) + 105}$.

We have

$$\lim_{t \to \infty} w_{\text{eff}}(t) = \frac{-7 + \sqrt{8\mu(2\mu - 9) + 105}}{4(\mu - 1)}, \quad \lim_{t \to \infty} \Omega_{\text{m}}(t) = \frac{5 - \sqrt{8\mu(2\mu - 9) + 105}}{2(\mu - 2)}, \quad (155)$$

such that $-1 \leq \lim_{t \to \infty} w_{\text{eff}}(t) \leq -1/3$ for $\mu \leq \frac{5}{2}$ and $0 \leq \lim_{t \to \infty} \Omega_{\text{m}}(t) \leq 1$ for $1 \leq \mu \leq \frac{5}{2}$. For large t, we have the asymptotic solution

$$H(t) \simeq \frac{1}{6t}\left(9 - 2\mu + \sqrt{8\mu(2\mu - 9) + 105}\right), \quad (156)$$

and

$$\lim_{t \to \infty} \alpha(t) = \frac{1}{6}\left(9 - 2\mu + \sqrt{8\mu(2\mu - 9) + 105}\right) \geq 0, \quad (157)$$

where $\alpha(t) = tH$ is the age parameter.

Finally, combining the solution of Bernoulli's Equation (137) and inequality (140) and then solving the differential inequality (141) and approximating the different quadrature, we have

$$E(z) \simeq \frac{1}{\alpha_0}\left[\frac{1}{9}\left((9 - 2\mu)\left(1 - (1+z)^{-3}\right) + 3m_0^{\frac{1}{2}}\right)^2 (1+z)^6 + A^2\right]^{\frac{1}{2}} (1+z)^{\frac{3}{\sqrt{9A^2 + (9-2\mu)^2}}}$$

and

$$t(z) \simeq t_0(1+z)^{-\frac{3}{\sqrt{9A^2 + (9-2\mu)^2}}},$$

as $z \to -1$, where α_0 is defined by (132), A is defined by (147), satisfying inequality (142) and $m_0 = \alpha_0^2 - A^2$. This is an accurate approximation of $E(z)$ as $z \to -1$ provided $2 \leq \mu \leq \frac{1}{10}\left(63 + \sqrt{849}\right) \lesssim 9.21376$. Moreover, $A \in [0, A_+]$ for $2 \leq \mu \leq 3.25162$ or $7.59791 \leq \mu \leq 9.21376$.

4. Cosmological Constraints

In this section, to study the capability of the models obtained in fractional cosmology to describe the late-time accelerated Universe expansion, we shall constrain the free parameters with the SNe Ia data and OHD. In particular, for the first one, we consider the Pantheon sample [101], which consists of 1048 supernovae data points in the redshift range $0.01 \leq z \leq 2.3$. On the other hand, we consider the OHD compiled by Magaña et al. [102], which consists of 51 data points in the redshift range $0.07 \leq z \leq 2.36$.

For the constraints, we compute the best-fit parameters and their respective confidence regions at $1\sigma(68.3\%)$, $2\sigma(95.5\%)$ and $3\sigma(99.7\%)$ confidence levels (CLs) with the affine-invariant Markov chain Monte Carlo (MCMC) method [103], implemented in the pure-Python code emcee [104] by setting 35 chains or "walkers". As a convergence test, we computed the autocorrelation time τ_{corr} of the chains provided by the emcee module at every 50th step. Hence, if the current step is larger than $50\tau_{corr}$ and the values of τ_{corr}

changed by less than 1%, then we will consider that the chains are converged and the constraint is stopped. The first $5\tau_{corr}$ steps are thus discarded as "burn-in" steps. This convergence test was complemented with the calculation of the mean acceptance fraction, which must have a value between 0.2 and 0.5 [104] and can be modified by the stretch move provided by the emcee module.

For this Bayesian statistical analysis, we need to construct the following Gaussian likelihood:

$$\mathcal{L} = \mathcal{N} \exp\left(-\frac{\chi_I^2}{2}\right), \tag{158}$$

where $\mathcal{N}$ is a normalization constant, which does not influence the MCMC analysis, and χ_I^2 is the merit function of each dataset considered, i.e., *I* stands for SNe Ia, OHD and their joint analysis. In the following subsections, we will briefly describe the construction of the merit function of each dataset, and we will present the main results and discussions.

4.1. Observational Hubble Parameter Data

The merit function for the OHD is constructed as

$$\chi_{OHD}^2 = \sum_{i=1}^{51} \left[\frac{H_i - H_{th}(z_i, \theta)}{\sigma_{H,i}}\right]^2, \tag{159}$$

where H_i is the observational Hubble parameter at redshift z_i with an associated error $\sigma_{H,i}$, all of them provided by the OHD sample, H_{th} is the theoretical Hubble parameter at the same redshift and θ encompasses the free parameters of the model under study. It is important to mention that the current value of the Hubble parameter, H_0, is a free parameter of the model, which for the constraint is written as $H_0 = 100\frac{\text{km/s}}{\text{Mpc}}h$, where h is dimensionless. Considering that we expect a value of H_0 between the value obtained from Planck CMB of $H_0 = 67.4$ [80] for the ΛCDM model and the value obtained by A. G. Riess et al. of $H_0 = 74.03$ [81] in a model-independent way, then we consider for h the flat prior $h \in F(0.4, 1)$.

4.2. Type Ia Supernovae Data

Similarly to the OHD, the merit function for the SNe Ia data is constructed as

$$\chi_{SNe}^2 = \sum_{i=1}^{1048} \left[\frac{\mu_i - \mu_{th}(z_i, \theta)}{\sigma_{\mu,i}}\right]^2, \tag{160}$$

where μ_i is the observational distance modulus of each SNe Ia at redshift z_i with an associated error $\sigma_{\mu,i}$, μ_{th} is the theoretical distance modulus for each SNe Ia at the same redshift and θ encompasses the free parameters of the model under study. Following this line, for a spatially flat FLRW spacetime, the theoretical distance modulus is given by

$$\mu_{th}(z_i, \theta) = 5\log_{10}\left[\frac{d_L(z_i, \theta)}{\text{Mpc}}\right] + \bar{\mu}, \tag{161}$$

where $\bar{\mu} = 5\left[\log_{10}(c) + 5\right]$ and where c is the speed of light given in units of km/s. The above expression relates the merit function with the theoretical Hubble parameter through the luminosity distance, d_L, as follows

$$d_L(z_i, \theta) = (1 + z_i)\int_0^{z_i} \frac{dz'}{H_{th}(z', \theta)}. \tag{162}$$

On the other hand, the distance estimator used in the Pantheon sample is obtained by a modified version of Tripp's formula [105], with two of the three nuisance parameters

calibrated to zero with the BEAMS with bias correction (BBC) method [106]. Hence, the observational distance modulus for each SNe Ia reads

$$\mu_i = m_{B,i} - \mathcal{M}, \tag{163}$$

where $m_{B,i}$ is the corrected apparent B-band magnitude of a fiducial SNe Ia at redshift z_i with an associated error $\sigma_{m_B,i}$, all of them provided by the Pantheon sample (currently available online in the GitHub repository https://github.com/dscolnic/Pantheon (accessed on 28 April 2023). The corrected apparent B-band magnitude $m_{B,i}$ for each SNe Ia with their respective redshifts z_i and errors $\sigma_{m_B,i}$ are available in the document *lcparam_full_long.txt*), and $\mathcal{M}$ is a nuisance parameter which must be jointly estimated with the free parameters θ of the theoretical model. Furthermore, the Pantheon sample provides the systematic uncertainties in the BBC approach, $\mathbf{C}_{sys}$ (currently available online in the GitHub repository https://github.com/dscolnic/Pantheon (accessed on 28 April 2023) in the document *sys_full_long.txt*). Therefore, we can rewrite the merit function (160) in matrix notation (denoted by bold symbols as)

$$\chi^2_{SNe} = \mathbf{M}(z,\theta,\mathcal{M})^{\dagger}\mathbf{C}^{-1}\mathbf{M}(z,\theta,\mathcal{M}), \tag{164}$$

where $[\mathbf{M}(z,\theta,\mathcal{M})]_i = m_{B,i} - \mu_{th}(z_i,\theta) - \mathcal{M}$ and $\mathbf{C} = \mathbf{D}_{stat} + \mathbf{C}_{sys}$ is the total uncertainty covariance matrix, where $\mathbf{D}_{stat} = diag(\sigma^2_{m_B,i})$ is the statistical uncertainty of m_B.

Finally, one can marginalize over the nuisance parameters $\bar{\mu}$ and $\mathcal{M}$ by defining $\bar{\mathcal{M}} = \bar{\mu} + \mathcal{M}$. Then, the merit function (164) can be expanded as [107]

$$\chi^2_{SNe} = A(z,\theta) - 2B(z,\theta)\bar{\mathcal{M}} + C\bar{\mathcal{M}}^2, \tag{165}$$

where

$$A(z,\theta) = \mathbf{M}(z,\theta,\bar{\mathcal{M}}=0)^{\dagger}\mathbf{C}^{-1}\mathbf{M}(z,\theta,\bar{\mathcal{M}}=0), \tag{166}$$

$$B(z,\theta) = \mathbf{M}(z,\theta,\bar{\mathcal{M}}=0)^{\dagger}\mathbf{C}^{-1}\mathbf{1}, \tag{167}$$

$$C = \mathbf{1}\mathbf{C}^{-1}\mathbf{1}. \tag{168}$$

Therefore, by minimizing the expanded merit function (165) with respect to $\bar{\mathcal{M}}$, $\bar{\mathcal{M}} = B(z,\theta)/C$ is obtained and the expanded merit is function reduced to

$$\chi^2_{SNe} = A(z,\theta) - \frac{B(z,\theta)^2}{C}, \tag{169}$$

which depends only on the free parameters of the theoretical model.

It is essential to mention that the expanded and minimized merit function (169) provides the same information as the merit function (164). This is a consequence of the fact that the best-fit parameters minimize the merit function. Therefore, the evaluation of the best-fit parameters in the merit function can be used as an indicator of the goodness of the fit independently of the dataset used; the smaller the value of χ^2_{min}, the better the fit.

4.3. Joint Analysis and Theoretical Hubble Parameter Integration

The merit function for the joint analysis is constructed directly as

$$\chi^2_{joint} = \chi^2_{OHD} + \chi^2_{SNe}, \tag{170}$$

with χ^2_{OHD} and χ^2_{SNe} given by Equations (159) and (169), respectively. Following this line, note how in the merit function of the two datasets, the respective model is considered through the (theoretical) Hubble parameter as a function of the redshift (see Equations (159) and (162)). Hence, for the constraint, we numerically integrate the sys-

tem given by Equations (128) and (129), which represents a system for the variables (α, t) as a function of $s = -\ln(1 + z)$, and for which we consider the initial conditions $\alpha(s = 0) \equiv \alpha_0 = t_0 H_0$ and $t(s = 0) \equiv t_0 = \alpha_0/H_0$. Then, the Hubble parameter is obtained numerically by $H_{th}(z) = \alpha(z)/t(z)$. For this integration, we consider the NumbaLSODA code, a python wrapper of the LSODA method in ODEPACK to C+ (currently available online in the GitHub repository https://github.com/Nicholaswogan/numbalsoda (accessed on 28 April 2023)). Furthermore, for further comparison, we also constrain the free parameters of the ΛCDM model, whose respective Hubble parameter as a function of the redshift is given by

$$H(z) = H_0 \sqrt{\Omega_{m,0}(1 + z)^3 + 1 - \Omega_{m,0}}. \tag{171}$$

Finally, based on the analysis made in Section 3.5, we consider the parameterization given by Equation (132) for the free parameter α_0. Therefore, the free parameters of the fractional cosmological model are $\theta = \{h, \mu, \epsilon_0\}$ and the free parameters of the ΛCDM model are $\theta = \{h, \Omega_{m,0}\}$. For the free parameters μ, ϵ_0 and $\Omega_{m,0}$, we consider the following flat priors: $\mu \in F(1,4)$, $\epsilon_0 \in F(-0.1, 0.1)$ and $\Omega_{m,0} \in F(0,1)$. It is important to mention that due to a degeneracy between H_0 and $\mathcal{M}$, the SNe Ia data are not able to constrain the free parameter h (as a reminder, $H_0 = 100 \frac{\text{km/s}}{\text{Mpc}} h$), contrary to the case for the OHD and, consequently, in the joint analysis. Thus, the posterior distribution of h for the SNe Ia data is expected to cover all the prior distributions. On the other hand, the prior is chosen as ϵ_0 because ϵ_0 is a measure of the limiting value of the relative error in the age parameter tH when it is approximated by $t_0 H_0$ as given by Equation (132). For the mean value $\epsilon_0 = 0$, we acquire $\alpha_0 = \frac{1}{6}(-2\mu + r + 9)$, which implies $c = 0$. Then, we have the leading term for $E(z)$ defined by (133). The lower prior of μ is because the Hubble parameter (22) becomes negative when $\mu < 1$ in the absence of matter, as we can see from Section 2.3.

4.4. Results and Discussion

In Table 2, we present the total steps, the mean acceptance fraction and the autocorrelation time, τ_{corr}, of each free parameter obtained when the convergence test is fulfilled during our MCMC analysis for both the fractional cosmological model and the ΛCDM model. The values of the mean acceptance fraction are obtained for a value of the stretch move of $a = 7$ for the ΛCDM model and $a = 3.5$ for the fractional cosmological model.

Table 2. The total number of steps, means acceptance fraction (MAF) and autocorrelation time, τ_{corr}, for the free parameters of the fractional cosmological model and the ΛCDM model. These values are obtained when the convergence test described in Section 4 is fulfilled for an MCMC analysis with 35 chains, a value of the stretch move of $a = 7$ for the ΛCDM model and $a = 3.5$ for the fractional cosmological model and for the flat priors $h \in F(0.4, 1)$, $\Omega_{m,0} \in F(0,1)$, $\mu \in F(1,4)$ and $\epsilon_0 \in F(-0.1, 0.1)$.

Data	Total Steps	MAF	τ_{corr}			
			h	$\Omega_{m,0}$	μ	ϵ_0
ΛCDM model						
SNe Ia	1300	0.328	24.0	20.8	$\cdots$	$\cdots$
OHD	950	0.364	16.1	15.4	$\cdots$	$\cdots$
SNe Ia + OHD	850	0.364	15.4	16.5	$\cdots$	$\cdots$
Fractional cosmological model						
SNe Ia	5250	0.339	50.9	$\cdots$	104.3	69.9
OHD	3150	0.377	35.9	$\cdots$	62.3	58.4
SNe Ia + OHD	1900	0.413	27.8	$\cdots$	33.8	32.1

The best-fit values of the free parameters space for the ΛCDM model and the fractional cosmological model, obtained for the SNe Ia data, OHD and in their joint analysis, with their corresponding χ^2_{min} criteria, are presented in Table 3. The uncertainties correspond to 1σ,

2σ and 3σ CL. In Figures 2 and 3, we depict the posterior distribution and joint admissible regions of the free parameter space of the ΛCDM model and the fractional cosmological model, respectively. The joint admissible regions correspond to 1σ, 2σ and 3σ CL. Due to the degeneracy between H_0 and $\mathcal{M}$, the distribution of h for the SNe Ia data was not represented in its full parameter space.

Table 3. Best-fit values and χ^2_{min} criteria for the fractional cosmological model with free parameters h, μ and ϵ_0 and for the ΛCDM model with free parameters h and $\Omega_{m,0}$. The values were obtained by the MCMC analysis described in Section 4 for the SNe Ia data, OHD and their joint analysis. The uncertainties presented correspond to $1\sigma(68.3\%)$, $2\sigma(95.5\%)$ and $3\sigma(99.7\%)$ confidence levels (CLs), respectively. The ΛCDM model is used as a reference model.

Data	Best-Fit Values				
	h	$\Omega_{m,0}$	μ	$\epsilon_0 \times 10^2$	χ^2_{min}
			ΛCDM model		
SNe Ia	$0.692^{+0.209\ +0.296\ +0.307}_{-0.120\ -0.278\ -0.292}$	$0.299^{+0.022\ +0.046\ +0.068}_{-0.021\ -0.042\ -0.059}$	. . .	. . .	1026.9
OHD	$0.706^{+0.012\ +0.024\ +0.035}_{-0.012\ -0.024\ -0.036}$	$0.259^{+0.018\ +0.038\ +0.059}_{-0.017\ -0.033\ -0.047}$	. . .	. . .	27.5
SNe Ia + OHD	$0.696^{+0.010\ +0.020\ +0.029}_{-0.010\ -0.020\ -0.029}$	$0.276^{+0.014\ +0.030\ +0.043}_{-0.014\ -0.027\ -0.040}$	. . .	. . .	1056.3
			Fractional cosmological model		
SNe Ia	$0.696^{+0.215\ +0.293\ +0.302}_{-0.204\ -0.284\ -0.295}$	. . .	$1.340^{+0.492\ +2.447\ +2.651}_{-0.245\ -0.328\ -0.339}$	$1.976^{+0.599\ +1.133\ +1.709}_{-0.905\ -1.848\ -2.067}$	1028.1
OHD	$0.675^{+0.013\ +0.029\ +0.041}_{-0.008\ -0.015\ -0.021}$	. . .	$2.239^{+0.449\ +0.908\ +1.386}_{-0.457\ -0.960\ -1.190}$	$0.865^{+0.395\ +0.650\ +0.793}_{-0.407\ -0.657\ -0.773}$	29.7
SNe Ia + OHD	$0.684^{+0.011\ +0.021\ +0.031}_{-0.010\ -0.020\ -0.027}$	. . .	$1.840^{+0.343\ +1.030\ +1.446}_{-0.298\ -0.586\ -0.773}$	$1.213^{+0.216\ +0.383\ +0.482}_{-0.310\ -0.880\ -1.057}$	1061.1
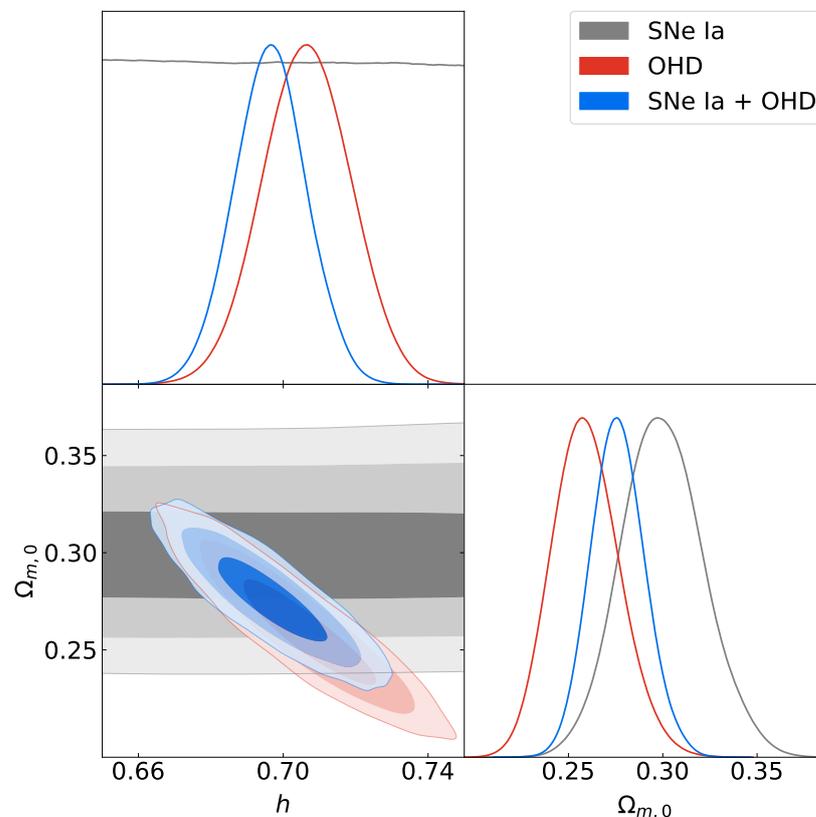
Figure 2. Posterior distribution and joint admissible regions of the free parameters h and $\Omega_{m,0}$ for the ΛCDM model, obtained by the MCMC analysis described in Section 4. The admissible joint regions correspond to $1\sigma(68.3\%)$, $2\sigma(95.5\%)$ and $3\sigma(99.7\%)$ of confidence level (CL), respectively. The best-fit values for each model free parameter are shown in Table 3.
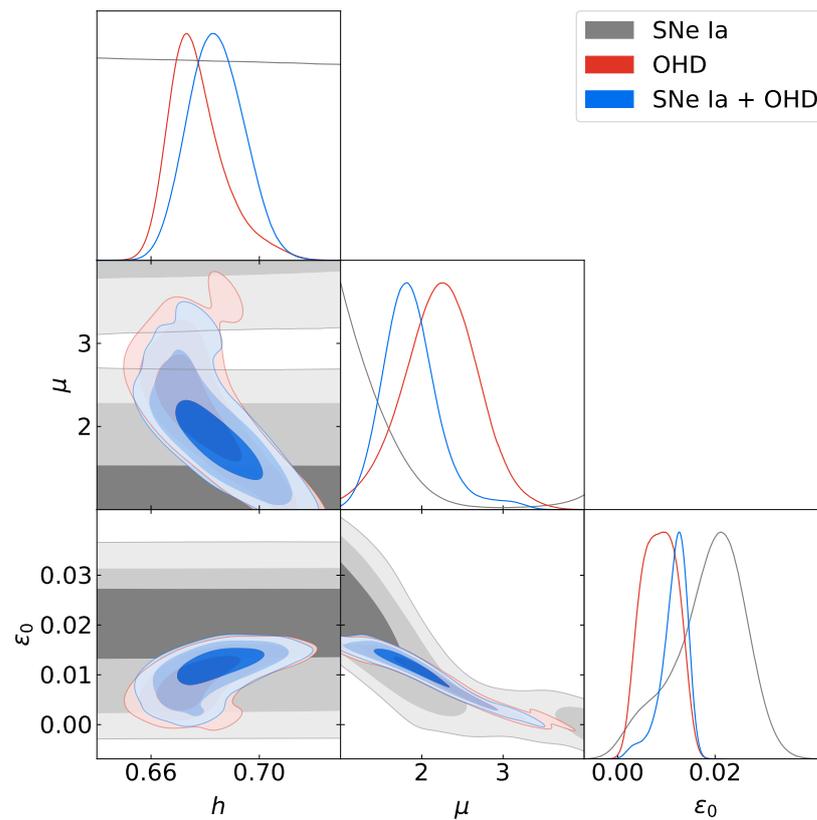
Figure 3. Posterior distribution and joint admissible regions of the free parameters h, μ and ϵ_0 for the fractional cosmological model, obtained by the MCMC analysis described in Section 4. The admissible joint regions correspond to $1\sigma(68.3\%)$, $2\sigma(95.5\%)$ and $3\sigma(99.7\%)$ confidence levels (CLs), respectively. The best-fit values for each model free parameter are shown in Table 3.

From the values for the χ^2_{min} criteria presented in Table 3, it is possible to see that the ΛCDM model is the best model to constrain the SNe Ia data, OHD and SNe Ia + OHD data. Nevertheless, the fractional cosmological model studied in this paper exhibits values of the χ^2_{min} criteria close to the values of the ΛCDM model, with differences of 1.2 for the SNe Ia data, 2.2 for the OHD data and 4.8 for their joint analysis. Thus, this fractional cosmological model is suitable for describing the SNe Ia and OHD data, as can be seen from Figures 4 and 5, which are characterized by accounting for a universe that experiences a transition between a deceleration expansion phase and an accelerated one. Therefore, fractional cosmology can be considered an alternative valid cosmological model to describe the late-time Universe. It is essential to mention that the core of this work is to probe this possibility by studying a particular model; the ΛCDM model is used only as a reference model for this aim.

The analysis of the SNe Ia data leads to $h = 0.696^{+0.302}_{-0.295}$, $\mu = 1.340^{+2.651}_{-0.339}$ and $\epsilon_0 = \left(1.976^{+1.709}_{-2.067}\right) \times 10^{-2}$, which are the best-fit values at 3σ CL. In this case, the value obtained for h cannot be considered as a best fit due to the degeneracy between H_0 and $\mathcal{M}$. On the other hand, the lower limit of the best fit for μ is very close to 1. That is because the posterior distribution for this parameter is close to this value, as seen from Figure 3. This indicates that a value of the SNe Ia data prefers $\mu < 1$, but, as a reminder, this value leads to a negative Hubble parameter in the absence of matter. However, as can be seen from the same Figure 3, the posterior distribution for these parameters is multi-modal (this explains the large value of τ_{corr} presented in Table 2) and, therefore, it is possible to obtain a best-fit value that satisfies $\mu > 1$. It is important to mention that the OHD and the joint analysis do not experience this issue, which allows us to maintain the validity of the prior used for μ.
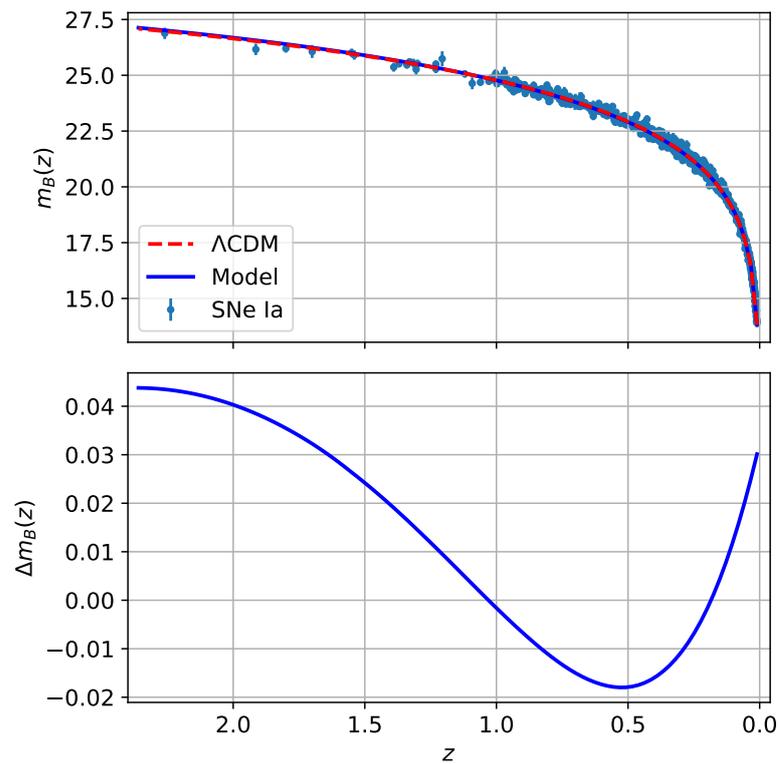
Figure 4. (**Top panel**) Theoretical apparent B-band magnitude for the ΛCDM model (red dashed line) and the fractional cosmological model (solid blue line) as a function of the redshift z, contrasted with the pantheon dataset. (**Bottom panel**) Variation in the theoretical apparent B-band magnitude of the fractional cosmological model compared to the ΛCDM model as a function of the redshift z. The curve is obtained through the expression $\Delta m_B = m_{B,Model} - m_{B,\Lambda CDM}$. The figures were obtained using the best-fit values for the SNe Ia+OHD data presented in Table 3.
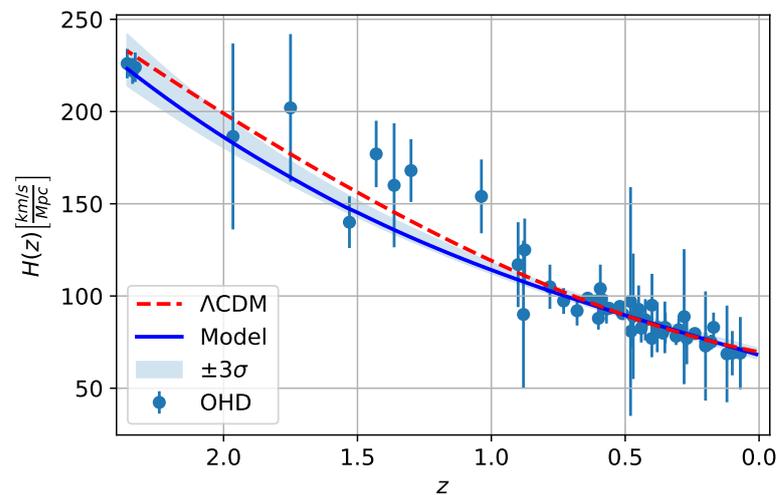
Figure 5. Theoretical Hubble parameter for the ΛCDM model (red dashed line) and the fractional cosmological model (solid blue line) as a function of the redshift z, contrasted with the OHD sample. The shaded curve represents the confidence region of the Hubble parameter for the fractional cosmological model at a $3\sigma(99.7\%)$ confidence level (CL). The figure was obtained using the best-fit values for the SNe Ia+OHD data presented in Table 3.

On the other hand, the analysis from OHD leads to $h = 0.675^{+0.041}_{-0.021}$, $\mu = 2.239^{+1.386}_{-1.190}$ and $\epsilon_0 = \left(0.865^{+0.793}_{-0.773}\right) \times 10^{-2}$, which are the best-fit values at 3σ CL. In this case, note how the OHD can properly constrain the free parameters h, μ and ϵ_0, i.e., we obtain the best

fit for the priors considered in our MCMC analysis. Furthermore, note how the posterior distribution of μ includes the value of 1, as seen from Figure 3, but for a CL greater than 3σ.

Finally, the joint analysis with data from SNe Ia + OHD leads to $h = 0.684^{+0.031}_{-0.027}$, $\mu = 1.840^{+1.446}_{-0.773}$ and $\epsilon_0 = \left(1.213^{+0.482}_{-1.057}\right) \times 10^{-2}$, which are the best-fit values at 3σ CL. Focusing our analysis on these results, we can conclude that the region in which $\mu > 2$ is not ruled out by observations. On the other hand, these best-fit values lead to an age of the Universe with a value of $t_0 = \alpha_0/H_0 = 25.62^{+6.89}_{-4.46}$ Gyrs at 3σ CL. Universe age is roughly double the one of the ΛCDM models, and is also in disagreement with the value obtained with globular clusters, with a value of $t_0 = 13.5^{+0.16}_{-0.14} \pm 0.23$ [70]. This discrepancy is a distinction of fractional cosmology. This result also agrees with the analysis made in Section 8 of [61], where the best-fit μ-value was obtained from the reconstruction of $H(z)$ for different priors of μ. The results are summarized in Table 4. In [61], a set of 31 points obtained by differential age tools was considered, namely cosmic chronometers (CC), to represent the measurements of the Hubble parameter, which is cosmologically independent [69] (in the present research we consider the datasets from [102], which consists of 51 data points in the redshift range $0.07 \leq z \leq 2.36$, 20 more points as compared with [69]). The 1048 luminosity modulus measurements, known as the Pantheon sample, from Type Ia Supernovae cover the region $0.01 < z < 2.3$ [101]. In [61], it is unclear if the different priors used for μ lead to properly constraining μ. Their analysis is inconclusive because of their present different values of μ for the different priors used.

Table 4. The best-fit values (μ, t_0) for different priors of μ derived in [61].

Prior	μ	t_0
$0 < \mu < 1$	0.50	41.30 Gyrs
$1 < \mu < 3$	1.71	27.89 Gyrs
$0 < \mu < 3$	1.15	33.66 Gyrs

In order to establish that this fractional cosmological model can describe a universe that experiences a transition from a decelerated expansion phase to an accelerated one, we computed the deceleration parameter $q = -1 - \dot{H}/H^2$, using the Riccati Equation (35), which leads to

$$q(\alpha(s)) = 2 + \frac{2(\mu - 4)}{\alpha(s)} - \frac{(\mu - 2)(\mu - 1)}{\alpha^2(s)}. \tag{172}$$

Following this line, in Figure 6, we depict the deceleration parameter for the fractional cosmological model as a function of the redshift z obtained from the best-fit values for the SNe Ia+OHD data presented in Table 3, with an error band at 3σ CL. We also depict the deceleration parameter for the ΛCDM model as a reference model. From this figure, we can conclude that the fractional cosmological model effectively experiences this transition at $z_t \gtrsim 1$, with the characteristic that $z_t > z_{t,\Lambda CDM}$, where $z_{t,\Lambda CDM}$ is the transition redshift of the ΛCDM model. Furthermore, the current deceleration parameter of the fractional cosmological model is $q_0 = -0.37^{+0.08}_{-0.11}$ at 3σ CL. On the other hand, in Figures 7 and 8, we depict the matter density and fractional density parameters for the fractional cosmological model (the last one interpreted as dark energy), respectively, as a function of the redshift z for the best-fit values for the SNe Ia+OHD data presented in Table 3, with an error band at 1σ CL. We depict the matter density and dark energy density parameters in both figures for the ΛCDM model. From Figure 7, we can see that the matter density parameter for the fractional cosmological model, obtained from Equation (126), presents significant uncertainties, which could be a consequence of their reconstruction from a Hubble parameter that does not take into account any EoS. In this sense, the current value of this matter density parameter at 1σ CL is $\Omega_{m,0} = 0.531^{+0.195}_{-0.260}$, a value that is in agreement with the asymptotic value obtained from Equation (155) of $\Omega_{m,t\to\infty} = 0.519^{+0.199}_{-0.262}$, computed at 1σ CL for the best-fit values for the SNe Ia+OHD data presented in Table 3. Therefore, this larger value of $\Omega_{m,0}$ for the fractional cosmological model can, in principle, explain

the lower value of the current deceleration parameter q_0 and the excess of matter in the effective term $\rho_{\text{frac}} = 3(\mu - 1)t^{-1}H$ with $\Omega_{\text{frac}}(\alpha(s)) = (\mu - 1)/\alpha(s)$ (see Section 2.6). Note that the current value $\Omega_{\text{frac},0}$ can be interpreted as the dark energy density parameter for the fractional cosmological model as $\Omega_{\text{frac},0} = 0.469^{+0.260}_{-0.195}$, which satisfies the condition $\Omega_{m,0} + \Omega_{\text{frac},0} = 1$.
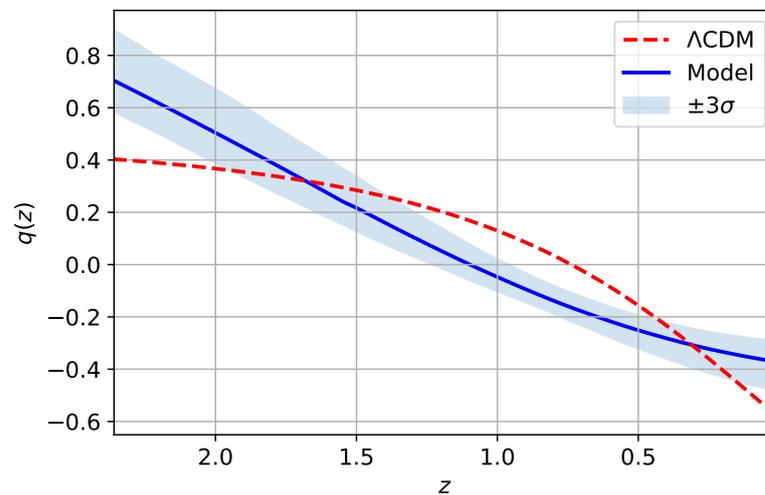
Figure 6. Deceleration parameters for the ΛCDM model (red dashed line) and the fractional cosmological model (solid blue line) as a function of the redshift z. The shaded curve represents the confidence region of the deceleration parameter for the fractional cosmological model at a $3\sigma(99.7\%)$ confidence level (CL). The figure was obtained using the best-fit values for the SNe Ia+OHD data presented in Table 3.
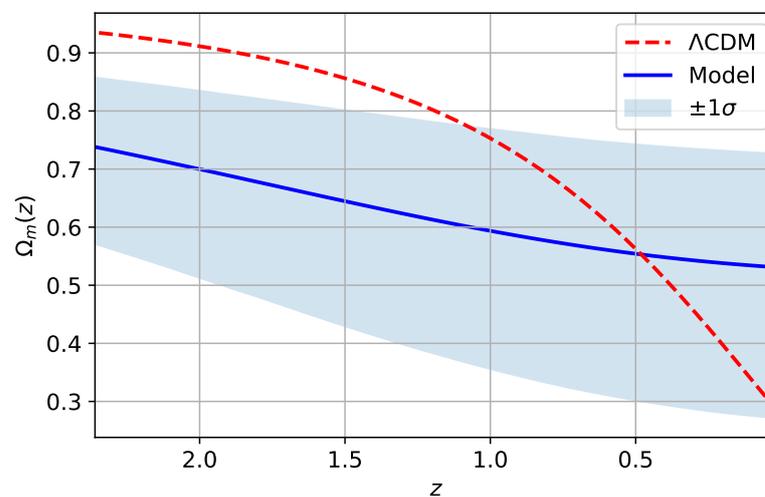
Figure 7. Matter density parameters for the ΛCDM model (red dashed line) and the fractional cosmological model (solid blue line) as a function of the redshift z. The shaded curve represents the confidence region of the matter density parameter for the fractional cosmological model at a $1\sigma(68.3\%)$ confidence level (CL). The figure was obtained using the best-fit values for the SNe Ia+OHD data presented in Table 3.
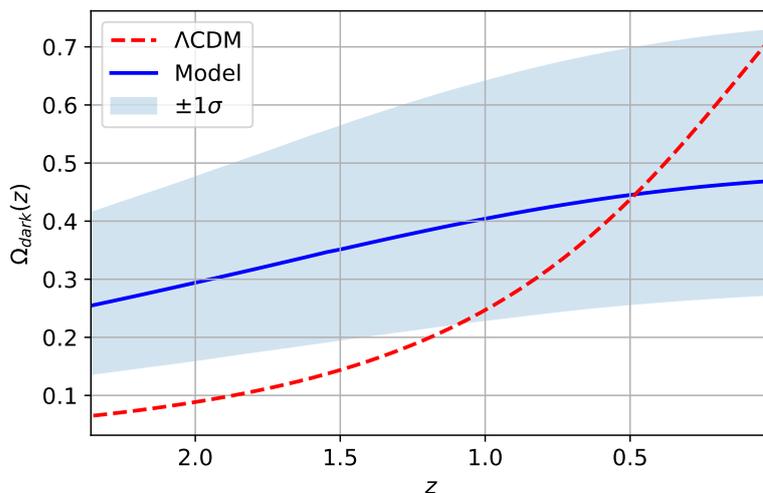
Figure 8. Dark energy density parameters for the ΛCDM model (red dashed line) and the fractional cosmological model (solid blue line) as a function of the redshift z. The shaded curve represents the confidence region of the dark energy density parameter for the fractional cosmological model at a $1\sigma(68.3\%)$ confidence level (CL). The figure was obtained using the best-fit values for the SNe Ia+OHD data presented in Table 3.

Finally, we compute the cosmographic parameter known as the jerk, which quantifies if the fractional cosmological model tends to Λ or if it another kind of DE, which can be written as

$$j(s) = q(s)(2q(s) + 1) - \frac{dq(s)}{ds}, \tag{173}$$

where q is given by Equation (172). Hence,

$$j(\alpha(s)) = \frac{12(\mu - 4)}{\alpha(s)} + \frac{(\mu - 21)\mu + 50}{\alpha(s)^2} - \frac{2(\mu - 3)(\mu - 2)(\mu - 1)}{\alpha(s)^3} + 10. \tag{174}$$

Figure 9 represents the jerks for the ΛCDM model (red dashed line) and the fractional cosmological model (solid blue line) as a function of the redshift z. The figure was obtained using the best-fit values for the SNe Ia+OHD data presented in Table 3 with an error band at 3σ CL, represented by a shaded region. A departure of more than a 3σ CL for the current value for ΛCDM shows an alternative cosmology with an effective dynamical equation of state for the Universe for late times in contrast to ΛCDM.

On the other hand, for the reconstruction of the $\mathbb{H}0(z)$ diagnostic [108] for the fractional cosmology, we define

$$\mathbb{H}0(z) = \frac{H(z)}{\sqrt{\Omega_{m,0}(1 + z)^3 + 1 - \Omega_{m,0}}}, \tag{175}$$

where the Hubble parameter is obtained numerically by $H(z) = H_{th}(z)$ as we explained before. Therefore, in Figure 10, we depict $\mathbb{H}0$ diagnostic for the ΛCDM model (red dashed line) and the fractional cosmological model (solid blue line) as a function of the redshift z. The figure was obtained using the best-fit values for the SNe Ia+OHD data presented in Table 3, with an error band at 3σ CL, represented by a shaded region. As a reminder, in both Figures 9 and 10, we also depict the jerk and the $\mathbb{H}0$ diagnostic for the ΛCDM model as a reference model.
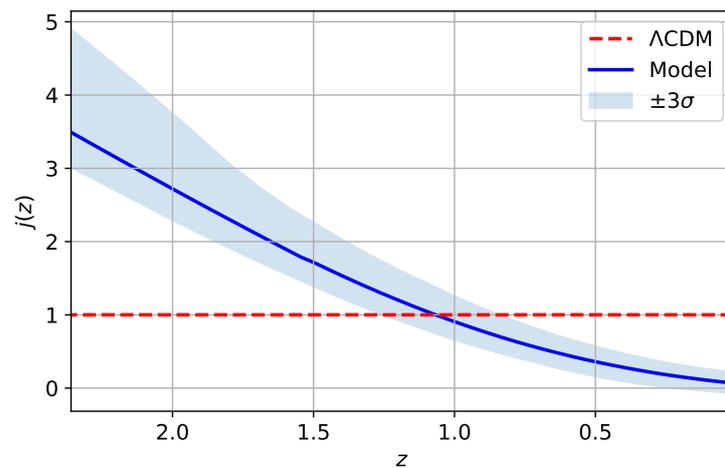
Figure 9. Jerks for the ΛCDM model (red dashed line) and the fractional cosmological model (solid blue line) as a function of the redshift z. The shaded curve represents the confidence region of the jerk for the fractional cosmological model at a $3\sigma(99.7\%)$ confidence level (CL). The figure was obtained using the best-fit values for the SNe Ia+OHD data presented in Table 3.
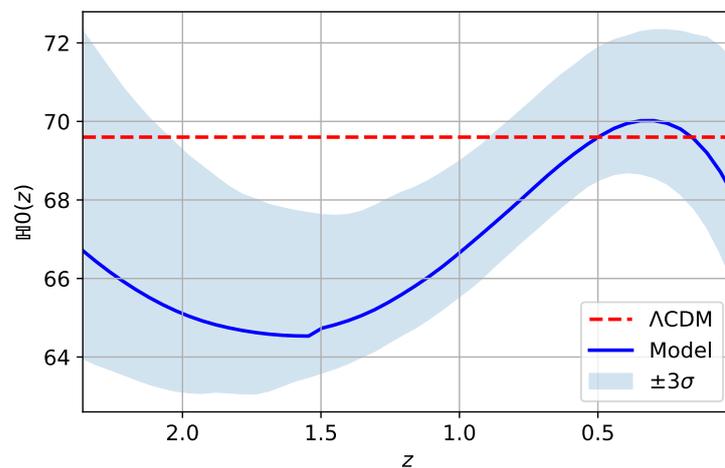
Figure 10. $\mathbb{H}0$ diagnostics for the ΛCDM model (red dashed line) and the fractional cosmological model (solid blue line) as a function of the redshift z. The shaded curve represents the confidence region of the $\mathbb{H}0$ diagnostic for the fractional cosmological model at a $3\sigma(99.7\%)$ confidence level (CL). The figure was obtained using the best-fit values for the SNe Ia+OHD data presented in Table 3.

5. Conclusions

In this paper, we investigated the cosmological applications of power-law solutions of the type $a = (t/t_0)^{\alpha_0}$ in fractional cosmology, where $\alpha_0 = t_0 H_0$ is the current age parameter. Additionally, given μ, the order of the fractional derivative, and w, the matter equation of state, we have imposed compatibility conditions which allow particular solutions to (μ, w). That means that any solution of power law type is indeed a particular exact solution of the system, e.g., solution (22) for $\rho = 0$; solution (74) for dust matter where α is defined by (71); solutions $H_{1,2}$ defined by (94), with $\alpha_{\pm}$ defined by (95) and where the compatibility conditions (97) and (98) are satisfied simultaneously for μ and w; and the solution (111) such that μ and w satisfy (112) and (113), respectively. However, they are not the general solution. Moreover, we are interested in an exact solution that gives the general solution of the system. For this purpose, we solved the Riccati equation (35) independent of the EoS, where the solution for the scale factor is a combination of power laws, i.e., (117). This solution is analyzed in Section 3.3.

Finally, combining the solution of Bernoulli's Equation (137) and the inequality (140), solving the differential inequality (141) and approximating the different quadrature, we have obtained the approximate analytical solution $E_{\text{approx}}(z)$ given by (153), and $t_{\text{approx}}(z)$ given by (154) as $z \to -1$, where α_0 is defined by (132), A is defined by (147) and satisfies (142) and $m_0 = \alpha_0^2 - A^2$. This is an accurate approximation of $E(z)$ as $z \to -1$ provided $2 \le \mu \le \frac{1}{10}\left(63 + \sqrt{849}\right) \lesssim 9.21376$.

Finally, we estimated the free parameters (α_0, μ) using cosmological data and the re-parameterization $H_0 = 100\frac{\text{km/s}}{\text{Mpc}}h$, $\alpha_0 = \frac{1}{6}\left(9 - 2\mu + \sqrt{8\mu(2\mu - 9) + 105}\right)(1 + 2\epsilon_0)$.

Separate analyses of the SNe Ia data and OHD, and the joint analysis with SNe Ia data + OHD, led, respectively, to $h = 0.696^{+0.302}_{-0.295}$, $\mu = 1.340^{+2.651}_{-0.339}$ and $\epsilon_0 = \left(1.976^{+1.709}_{-2.067}\right) \times 10^{-2}$; $h = 0.675^{+0.041}_{-0.021}$, $\mu = 2.239^{+1.386}_{-1.190}$ and $\epsilon_0 = \left(0.865^{+0.793}_{-0.773}\right) \times 10^{-2}$; and $h = 0.684^{+0.031}_{-0.027}$, $\mu = 1.840^{+1.446}_{-0.773}$ and $\epsilon_0 = \left(1.213^{+0.482}_{-1.057}\right) \times 10^{-2}$, where the best-fit values were calculated at 3σ CL. On the other hand, these best-fit values led to an age of the Universe with a value of $t_0 = \alpha_0/H_0 = 25.62^{+6.89}_{-4.46}$ Gyrs, a current deceleration parameter of $q_0 = -0.37^{+0.08}_{-0.11}$ (both at 3σ CL) and a current matter density parameter of $\Omega_{m,0} = 0.531^{+0.195}_{-0.260}$ at 1σ CL. Finding a Universe roughly twice as old as the one of ΛCDM is a distinction of fractional cosmology. Focusing our analysis on these results, we can conclude that the region in which $\mu > 2$ is not ruled out by observations. This region of a parameter is relevant because, in the absence of matter, fractional cosmology gives a power-law solution $a(t) = (t/t_0)^{\mu-1}$, which is accelerated for $\mu > 2$. We presented a fractional origin model that leads to an accelerated state without appealing to Λ or dark energy.

Author Contributions: Conceptualization, E.G. and G.L.; methodology, E.G., G.L. and G.F.-A.; software, E.G. and G.L.; validation, E.G., G.L. and G.F.-A.; formal analysis, E.G., G.L. and G.F.-A.; investigation, E.G., G.L. and G.F.-A.; resources, G.L.; writing—original draft preparation, G.L.; writing—review and editing, E.G., G.L. and G.F.-A.; visualization, E.G. and G.L.; supervision, G.L.; project administration, G.L.; funding acquisition, G.L. All authors have read and agreed to the published version of the manuscript.

Institutional Review Board Statement: Not applicable.

Informed Consent Statement: Not applicable.

Data Availability Statement: The data supporting this article can be found in Section 4.

Conflicts of Interest: The authors declare no conflict of interest. The funders had no role in the design of the study; in the collection, analyses, or interpretation of data; in the writing of the manuscript; or in the decision to publish the results.

References

1. Monje, C.A.; Chen, Y.Q.; Vinagre, B.M.; Xue, D.; Feliu-Batlle, V. *Fractional-Order Systems and Controls: Fundamentals and Applications*; Advances in Industrial Control; Springer: London, UK, 2010.
2. Tarasov, V.E. Review of Some Promising Fractional Physical Models. *Int. J. Mod. Phys. B* **2013**, 27, 13300053. [CrossRef]
3. Bandyopadhyay, B.; Kamal, S. *Stabilization and Control of Fractional Order Systems: A Sliding Mode Approach*; Lecture Notes in Electrical Engineering; Springer International Publishing: New York, NY, USA, 2014.
4. Padula, F.; Visioli, A. *Advances in Robust Fractional Control*; Springer International Publishing: New York, NY, USA, 2014.
5. Herrmann, R. *Fractional Calculus: An Introduction For Physicists*, 2nd ed.; World Scientific Publishing Company: Singapore, 2014.
6. Tarasov, V.E. *Applications in Physics, Part A*; De Gruyter Reference; De Gruyter: Berlin, Germany, 2019.

7.   Klafter, J.; Lim, S.C.; Metzler, R. *Fractional Dynamics: Recent Advances*; World Scientific: Singapore, 2012.
8.   Malinowska, A.B.; Odzijewicz, T.; Torres, D.F.M. *Advanced Methods in the Fractional Calculus of Variations*; Springer Briefs in Applied Sciences and Technology; Springer International Publishing: New York, NY, USA, 2015.
9.   Lorenzo, C.F.; Hartley, T.T. *The Fractional Trigonometry: With Applications to Fractional Differential Equations and Science*; Wiley: Hoboken, NJ, USA, 2016.
10.   West, B.J. Fractional Calculus and the Future of Science. *Entropy* **2021**, *23*, 1566. [CrossRef] [PubMed]
11.   Calcagni, G. Quantum field theory, gravity and cosmology in a fractal universe. *JHEP* **2010**, *03*, 120. [CrossRef]
12.   Calcagni, G. Fractal universe and quantum gravity. *Phys. Rev. Lett.* **2010**, *104*, 251301.
13.   Lim, S.C. Fractional derivative quantum fields at positive temperature. *Phys. A* **2006**, *363*, 269–281. [CrossRef]
14.   Lim, S.C.; Eab, C.H. Fractional quantum fields. In *Volume 5 Applications in Physics, Part B*; Tarasov, V.E., Ed.; De Gruyter: Berlin, Germany, 2019; pp. 237–256. [CrossRef]
15.   Moniz, P.V.; Jalalzadeh, S. *Challenging Routes in Quantum Cosmology*; World Scientific Publishing: Singapore, 2020. [CrossRef]
16.   Moniz, P.V.; Jalalzadeh, S. From Fractional Quantum Mechanics to Quantum Cosmology: An Overture. *Mathematics* **2020**, *8*, 313. [CrossRef]
17.   Rasouli, S.M.M.; Jalalzadeh, S.; Moniz, P.V. Broadening quantum cosmology with a fractional whirl. *Mod. Phys. Lett. A* **2021**, *36*, 2140005. [CrossRef]
18.   Jalalzadeh, S.; da Silva, F.R.; Moniz, P.V. Prospecting black hole thermodynamics with fractional quantum mechanics. *Eur. Phys. J. C* **2021**, *81*, 632. [CrossRef]
19.   Rami, E.N.A. Fractional dynamics, fractional weak bosons masses and physics beyond the standard model. *Chaos Solitons Fractals* **2009**, *41*, 2262–2270. [CrossRef]
20.   El-Nabulsi, R.A. Fractional Lagrangian Formulation of General Relativity and Emergence of Complex, Spinorial and Noncommutative Gravity. *Int. J. Geom. Methods Mod. Phys.* **2009**, *6*, 25–76. [CrossRef]
21.   El-Nabulsi, R.A. Modifications at Large Distances From Fractional and Fractal Arguments. *Fractals* **2010**, *18*, 185–190. [CrossRef]
22.   El-Nabulsi, A.R. The fractional white dwarf hydrodynamical nonlinear differential equation and emergence of quark stars. *Appl. Math. Comput.* **2011**, *218*, 2837–2849. [CrossRef]
23.   El-Nabulsi, R.A. Glaeske-Kilbas-Saigo fractional integration and fractional Dixmier trace. *Acta Math. Vietnam.* **2012**, *37*, 149–160.
24.   El-Nabulsi, R.A.; Wu, C.G. Fractional Complexified Field Theory from Saxena-Kumbhat Fractional Integral, Fractional Derivative of Order (α, β) and Dynamical Fractional Integral Exponent. *Afr. Diaspora J. Math. New Ser.* **2012**, *13*, 45–61.
25.   El-Nabulsi, R.A. Fractional derivatives generalization of Einstein's field equations. *Indian J. Phys.* **2013**, *87*, 195–200. [CrossRef]
26.   El-Nabulsi, R.A. Fractional elliptic operator of order 2/3 from Glaeske-Kilbas-Saigo fractional integral transform. *Funct. Anal. Approx. Comput* **2015**, *7*, 29–33.
27.   El-Nabulsi, R.A. A Cosmology Governed by a Fractional Differential Equation and the Generalized Kilbas-Saigo-Mittag–Leffler Function. *Int. J. Theor. Phys.* **2016**, *55*, 625–635. [CrossRef]
28.   El-Nabulsi, R.A. Finite two-point space without quantization on noncommutative space from a generalized fractional integral operator. *Complex Anal. Oper. Theory* **2018**, *12*, 1609–1616. [CrossRef]
29.   El-Nabulsi, R.A. On generalized fractional spin, fractional angular momentum, fractional momentum operators in quantum mechanics. *Few-Body Syst.* **2020**, *61*, 25. [CrossRef]
30.   Roberts, M.D. Fractional Derivative Cosmology. *SOP Trans. Theor. Phys.* **2014**, *1*, 310. [CrossRef]
31.   Vacaru, S.I. New Classes of Off-Diagonal Cosmological Solutions in Einstein Gravity. *Int. J. Theor. Phys.* **2010**, *49*, 2753–2776. [CrossRef]
32.   Vacaru, S.I. Fractional Nonholonomic Ricci Flows. *Chaos Solitons Fractals* **2012**, *45*, 1266–1276. [CrossRef]
33.   Vacaru, S.I. Fractional Dynamics from Einstein Gravity, General Solutions, and Black Holes. *Int. J. Theor. Phys.* **2012**, *51*, 1338–1359. [CrossRef]
34.   Shchigolev, V.K. Cosmological Models with Fractional Derivatives and Fractional Action Functional. *Commun. Theor. Phys.* **2011**, *56*, 389–396. [CrossRef]
35.   Jamil, M.; Momeni, D.; Rashid, M.A. Fractional Action Cosmology with Power Law Weight Function. *J. Phys. Conf. Ser.* **2012**, *354*, 012008. [CrossRef]
36.   Shchigolev, V.K. Cosmic Evolution in Fractional Action Cosmology. *Discontinuity Nonlinearity Complex* **2013**, *2*, 115–123. [CrossRef]
37.   Debnath, U.; Jamil, M.; Chattopadhyay, S. Fractional Action Cosmology: Emergent, Logamediate, Intermediate, Power Law Scenarios of the Universe and Generalized Second Law of Thermodynamics. *Int. J. Theor. Phys.* **2012**, *51*, 812–837. [CrossRef]
38.   El-Nabulsi, R.A. Gravitons in fractional action cosmology. *Int. J. Theor. Phys.* **2012**, *51*, 3978–3992. [CrossRef]
39.   El-Nabulsi, R.A. Non-minimal coupling in fractional action cosmology. *Indian J. Phys.* **2013**, *87*, 835–840. [CrossRef]
40.   El-Nabulsi, R.A. Nonstandard fractional exponential Lagrangians, fractional geodesic equation, complex general relativity, and discrete gravity. *Can. J. Phys.* **2013**, *91*, 618–622. [CrossRef]
41.   Debnath, U.; Chattopadhyay, S.; Jamil, M. Fractional action cosmology: Some dark energy models in emergent, logamediate, and intermediate scenarios of the universe. *J. Theor. Appl. Phys.* **2013**, *7*, 25. [CrossRef]
42.   Shchigolev, V.K. Fractional Einstein–Hilbert Action Cosmology. *Mod. Phys. Lett. A* **2013**, *28*, 1350056. [CrossRef]
43.   Calcagni, G. Multi-scale gravity and cosmology. *J. Cosmol. Astropart. Phys.* **2013**, *12*, 041. [CrossRef]

44. Shchigolev, V.K. Testing Fractional Action Cosmology. *Eur. Phys. J. Plus* **2016**, *131*, 256. [CrossRef]
45. Rami, E.N.A. Fractional action oscillating phantom cosmology with conformal coupling. *Eur. Phys. J. Plus* **2015**, *130*, 102. [CrossRef]
46. El-Nabulsi, R.A. Implications of the Ornstein-Uhlenbeck-like fractional differential equation in cosmology. *Rev. Mex. Fis.* **2016**, *62*, 240.
47. Calcagni, G.; Kuroyanagi, S.; Tsujikawa, S. Cosmic microwave background and inflation in multi-fractional spacetimes. *J. Cosmol. Astropart. Phys.* **2016**, *8*, 39. [CrossRef]
48. Calcagni, G. Multifractional theories: An unconventional review. *J. High Energy Phys.* **2017**, *3*, 138; Erratum in *J. High Energy Phys.* **2017**, *6*, 20. [CrossRef]
49. El-Nabulsi, R.A. Fractional Action Cosmology with Variable Order Parameter. *Int. J. Theor. Phys.* **2017**, *56*, 1159–1182. [CrossRef]
50. El-Nabulsi, R.A. Wormholes in fractional action cosmology. *Can. J. Phys.* **2017**, *95*, 605–609. [CrossRef]
51. Calcagni, G. Complex dimensions and their observability. *Phys. Rev. D* **2017**, *96*, 046001. [CrossRef]
52. Calcagni, G.; Kuroyanagi, S.; Marsat, S.; Sakellariadou, M.; Tamanini, N.; Tasinato, G. Quantum gravity and gravitational-wave astronomy. *J. Cosmol. Astropart. Phys.* **2019**, *10*, 012. [CrossRef]
53. Calcagni, G.; Kuroyanagi, S. Stochastic gravitational-wave background in quantum gravity. *J. Cosmol. Astropart. Phys.* **2021**, *3*, 19. [CrossRef]
54. Calcagni, G.; De Felice, A. Dark energy in multifractional spacetimes. *Phys. Rev. D* **2020**, *102*, 103529. [CrossRef]
55. Calcagni, G. Multifractional theories: An updated review. *Mod. Phys. Lett. A* **2021**, *36*, 2140006. [CrossRef]
56. Calcagni, G. Classical and quantum gravity with fractional operators. *Class. Quant. Grav.* **2021**, *38*, 165005; Erratum in *Class. Quant. Grav.* **2021**, *38*, 169601. [CrossRef]
57. Shchigolev, V.K. Fractional-order derivatives in cosmological models of accelerated expansion. *Mod. Phys. Lett. A* **2021**, *36*, 2130014. [CrossRef]
58. Jalalzadeh, S.; Costa, E.W.O.; Moniz, P.V. de Sitter fractional quantum cosmology. *Phys. Rev. D* **2022**, *105*, L121901. [CrossRef]
59. Landim, R.G. Fractional dark energy: Phantom behavior and negative absolute temperature. *Phys. Rev. D* **2021**, *104*, 103508. [CrossRef]
60. Landim, R.G. Fractional dark energy. *Phys. Rev. D* **2021**, *103*, 083511. [CrossRef]
61. García-Aspeitia, M.A.; Fernandez-Anaya, G.; Hernández-Almada, A.; Leon, G.; Magaña, J. Cosmology under the fractional calculus approach. *Mon. Not. R. Astron. Soc.* **2022**, *517*, 4813–4826. [CrossRef]
62. Micolta-Riascos, B.; Millano, A.D.; Leon, G.; Erices, C.; Paliathanasis, A. Revisiting Fractional Cosmology. *Fractal Fract.* **2023**, *7*, 149. [CrossRef]
63. Hernández-Almada, A.; Leon, G.; Magaña, J.; García-Aspeitia, M.A.; Motta, V. Generalized Emergent Dark Energy: Observational Hubble data constraints and stability analysis. *Mon. Not. R. Astron. Soc.* **2020**, *497*, 1590–1602. [CrossRef]
64. Leon, G.; Magaña, J.; Hernández-Almada, A.; García-Aspeitia, M.A.; Verdugo, T.; Motta, V. Barrow Entropy Cosmology: An observational approach with a hint of stability analysis. *J. Cosmol. Astropart. Phys.* **2021**, *12*, 032. [CrossRef]
65. Hernández-Almada, A.; Leon, G.; Magaña, J.; García-Aspeitia, M.A.; Motta, V.; Saridakis, E.N.; Yesmakhanova, K.; Millano, A.D. Observational constraints and dynamical analysis of Kaniadakis horizon-entropy cosmology. *Mon. Not. R. Astron. Soc.* **2022**, *512*, 5122–5134. [CrossRef]
66. Hernández-Almada, A.; Leon, G.; Magaña, J.; García-Aspeitia, M.A.; Motta, V.; Saridakis, E.N.; Yesmakhanova, K. Kaniadakis-holographic dark energy: Observational constraints and global dynamics. *Mon. Not. R. Astron. Soc.* **2022**, *511*, 4147–4158. [CrossRef]
67. Riess, A.G.; Filippenko, A.V.; Challis, P.; Clocchiatti, A.; Diercks, A.; Garnavich, P.M.; Gillil, R.L.; Hogan, C.J.; Jha, S.; Kirshner, R.P.; et al. Observational evidence from supernovae for an accelerating universe and a cosmological constant. *Astron. J.* **1998**, *116*, 1009–1038.
68. Perlmutter, S.; Aldering, G.; Goldhaber, G.; Knop, R.A.; Nugent, P.; Castro, P.G.; Deustua, S.; Fabbro, S.; Goobar, A.; Groom, D.E.; et al. Measurements of Ω and Λ from 42 high redshift supernovae. *Astrophys. J.* **1999**, *517*, 565–586.
69. Moresco, M.; Pozzetti, L.; Cimatti, A.; Jimenez, R.; Maraston, C.; Verde, L.; Thomas, D.; Citro, A.; Tojeiro, R.; Wilkinson, D. A 6% measurement of the Hubble parameter at $z \sim 0.45$: Direct evidence of the epoch of cosmic re-acceleration. *J. Cosmol. Astropart. Phys.* **2016**, *5*, 14. [CrossRef]
70. Valcin, D.; Jimenez, R.; Verde, L.; Bernal, J.L.; Wandelt, B.D. The age of the Universe with globular clusters: Reducing systematic uncertainties. *J. Cosmol. Astropart. Phys.* **2021**, *2021*, 17. [CrossRef]
71. Weinberg, S. The Cosmological Constant Problem. *Rev. Mod. Phys.* **1989**, *61*, 1–23. [CrossRef]
72. Carroll, S.M.; Press, W.H.; Turner, E.L. The Cosmological constant. *Ann. Rev. Astron. Astrophys.* **1992**, *30*, 499–542. [CrossRef]
73. Sahni, V.; Starobinsky, A.A. The Case for a positive cosmological Lambda term. *Int. J. Mod. Phys. D* **2000**, *9*, 373–444.
74. Peebles, P.J.E.; Ratra, B. The Cosmological Constant and Dark Energy. *Rev. Mod. Phys.* **2003**, *75*, 559–606.
75. Padmanabhan, T. Cosmological constant: The Weight of the vacuum. *Phys. Rept.* **2003**, *380*, 235–320.
76. Velten, H.E.S.; vom Marttens, R.F.; Zimdahl, W. Aspects of the cosmological "coincidence problem". *Eur. Phys. J. C* **2014**, *74*, 3160. [CrossRef]
77. Sadjadi, H.M.; Alimohammadi, M. Cosmological coincidence problem in interactive dark energy models. *Phys. Rev. D* **2006**, *74*, 103007. [CrossRef]

78. Zlatev, I.; Wang, L.M.; Steinhardt, P.J. Quintessence, cosmic coincidence, and the cosmological constant. *Phys. Rev. Lett.* **1999**, *82*, 896–899.

79. Riess, A.G.; Yuan, W.; Macri, L.M.; Scolnic, D.; Brout, D.; Casertano, S.; Jones, D.O.; Murakami, Y.; An G.S.; Breuval, L.; et al. A Comprehensive Measurement of the Local Value of the Hubble Constant with 1 km s^{-1} Mpc^{-1} Uncertainty from the Hubble Space Telescope and the SH0ES Team. *Astrophys. J. Lett.* **2022**, *934*, L7. [CrossRef]

80. Aghanim, N.; Akrami, Y.; Ashdown, M.; Aumont, J.; Baccigalupi, C.; Ballardini, M.; Banday, A.J.; Barreiro, R.B.; Bartolo, N.; Basak, S.; et al. Planck 2018 results. VI. Cosmological parameters. *Astron. Astrophys.* **2020**, *641*, A6; Erratum in *Astron. Astrophys.* **2021**, *652*, C4. [CrossRef]

81. Riess, A.G.; Casertano, S.; Yuan, W.; Macri, L.M.; Scolnic, D. Large Magellanic Cloud Cepheid Standards Provide a 1% Foundation for the Determination of the Hubble Constant and Stronger Evidence for Physics beyond ΛCDM. *Astrophys. J.* **2019**, *876*, 85.

82. Di Valentino, E.; Mena, O.; Pan, S.; Visinelli, L.; Yang, W.; Melchiorri, A.; Mota, D.F.; Riess, A.G.; Silk, J. In the realm of the Hubble tension—a review of solutions. *Class. Quant. Grav.* **2021**, *38*, 153001.

83. Basilakos, S.; Leon, G.; Papagiannopoulos, G.; Saridakis, E.N. Dynamical system analysis at background and perturbation levels: Quintessence in severe disadvantage comparing to ΛCDM. *Phys. Rev. D* **2019**, *100*, 043524.

84. Alho, A.; Uggla, C.; Wainwright, J. Perturbations of the Lambda-CDM model in a dynamical systems perspective. *J. Cosmol. Astropart. Phys.* **2019**, *9*, 45.

85. Wald, R.M. Asymptotic behavior of homogeneous cosmological models in the presence of a positive cosmological constant. *Phys. Rev. D* **1983**, *28*, 2118. [CrossRef]

86. Kitada, Y.; Maeda, K.I. Cosmic no-hair theorem in homogeneous spacetimes. *Vistas Astron.* **1993**, *37*, 461–464. [CrossRef]

87. Barrow, J.D.; Stein-Schabes, J. Inhomogeneous cosmologies with cosmological constant. *Phys. Lett. A* **1984**, *103*, 315–317. [CrossRef]

88. Maeda, K.I. Recent topics on the inflationary universe: Cosmic no hair conjecture. In Proceedings of the 2nd Workshop on Elementary Particle Picture of the Universe, Tsukuba, Japan, 4–6 February 1988; pp. 51–64.

89. Cotsakis, S.; Flessas, G. Generalized cosmic no hair theorems. *Phys. Lett. B* **1993**, *319*, 69–73. [CrossRef]

90. Capozziello, S.; De Ritis, R. Cosmic no-hair theorem in anisotropic, nonminimally coupled cosmologies. *Int. J. Mod. Phys. D* **1996**, *5*, 209–215. [CrossRef]

91. Bruni, M.; Mena, F.C.; Tavakol, R.K. Cosmic no hair: Nonlinear asymptotic stability of de Sitter universe. *Class. Quant. Grav.* **2002**, *19*, L23–L29.

92. Uchaikin, V.V. *Fractional Derivatives for Physicists and Engineers*; Higher Education Press: Beijing, China, 2013.

93. El-Nabulsi, R.A. Fractional unstable Euclidean universe. *Electron. J. Theor. Phys.* **2005**, *2*, 1–11.

94. El-Nabulsi, R.A. Accelerated universe dominated by holographic dark energy, supergravity inflationary potential. *Rom. J. Phys.* **2007**, *52*, 163–170.

95. El-Nabulsi, R.A. Cosmology with a fractional action principle. *Rom. Rep. Phys.* **2007**, *59*, 763–771.

96. El-Nabulsi, R.A. Increasing effective gravitational constant in fractional ADD brane cosmology. *Electron. J. Theor. Phys.* **2008**, *5*, 103–106.

97. Frederico, G.S.; Torres, D. Necessary Optimality Conditions for Fractional Action-like Problems with Intrinsic and Observer Times. *WSEAS Trans. Math.* **2008**, *7*, 6–11.

98. Wald, R.M. *General Relativity*; University of Chicago Press: Chicago, IL, USA, 2010.

99. Carroll, S.M. *Spacetime and Geometry*; Cambridge University Press: Cambridge, UK, 2019.

100. Carroll, S.; Carroll, S.M. *Spacetime and Geometry: An Introduction to General Relativity*; Addison Wesley: Boston, MA, USA, 2004.

101. Scolnic, D.M.; Jones, D.O.; Rest, A.; Pan, Y.C.; Chornock, R.; Foley, R.J.; Huber, M.E.; Kessler, R.; Narayan, G.; Riess, A.G.; et al. The Complete Light-curve Sample of Spectroscopically Confirmed SNe Ia from Pan-STARRS1 and Cosmological Constraints from the Combined Pantheon Sample. *Astrophys. J.* **2018**, *859*, 101.

102. Magaña, J.; Amante, M.H.; Garcia-Aspeitia, M.A.; Motta, V. The Cardassian expansion revisited: Constraints from updated Hubble parameter measurements and type Ia supernova data. *Mon. Not. R. Astron. Soc.* **2018**, *476*, 1036.

103. Goodman, J.; Weare, J. Ensemble samplers with affine invariance. *Commun. Appl. Math. Comput. Sci.* **2010**, *5*, 65–80. [CrossRef]

104. Foreman-Mackey, D.; Conley, A.; Meierjurgen Farr, W.; Hogg, D.W.; Lang, D.; Marshall, P.; Price-Whelan, A.; Sanders, J.; Zuntz, J. emcee: The MCMC Hammer. *Publ. Astron. Soc. Pac.* **2013**, *125*, 306.

105. Tripp, R. A two-parameter luminosity correction for Type IA supernovae. *Astron. Astrophys.* **1998**, *331*, 815.

106. Kessler, R.; Scolnic, D. Correcting Type Ia Supernova Distances for Selection Biases and Contamination in Photometrically Identified Samples. *Astrophys. J.* **2017**, *836*, 56.

107. Lazkoz, R.; Nesseris, S.; Perivolaropoulos, L. Exploring cosmological expansion parametrizations with the gold SnIa data set. *J. Cosmol. Astropart. Phys.* **2005**, *2005*, 010.

108. Krishnan, C.; Ó Colgáin, E.; Sheikh-Jabbari, M.M.; Yang, T. Running Hubble tension and a H0 diagnostic. *Phys. Rev. D* **2021**, *103*. [CrossRef]